

UNCLASSIFIED

AD NUMBER
ADB277452
NEW LIMITATION CHANGE
TO Approved for public release, distribution unlimited
FROM Distribution: Further dissemination only as directed by OSRD, Washington, DC 20301, 5 Jan 1946 or higher DoD authority.
AUTHORITY
OSRD, per DTIC Form 55, dtd 14 Nov 2002

THIS PAGE IS UNCLASSIFIED

OSRD
5607

UNCLASSIFIED

Division

NATIONAL DEFENSE RESEARCH COMMITTEE

of the

OFFICE OF SCIENTIFIC RESEARCH AND DEVELOPMENT

DISTRIBUTION STATEMENT F:

Further dissemination only as directed by

OSRD, WASHINGTON, DC
or higher DoD authority. 20301

5 JAN 1946

CLASSIFICATION CHANGED TO
UNCLASSIFIED
BY AUTHORITY OF DDA Ltr ADJ
GENERAL - WASH DC - AGHAI-PCW
9710-00 212V122
BY 2 Henry
107 May 63
OSRD No. 3564
Copy No. 29
LIBRARY
OSRD, MD.

20020214 008

OSRD
5607

Reproduced From
Best Available Copy

UNCLASSIFIED

UNCLASSIFIED

Progress Report

on

OSRD Report No. 5607

OSRD
5607

Studies of Shell Fragment Mass Distribution

Part I

Navy 3"/50 A.A. Projectiles, Mk. 27-3 and Mk. 31-1

from the

Explosives Research Laboratory

Bruceton, Pennsylvania

Investigation Group:

D. P. MacDougall, Deputy Research Director

W. K. Hall

J. F. Lemons, Group Leader

M. A. Paul, Research Supervisor

Report prepared by:

Report approved by:

M. A. Paul and W. K. Hall

D. P. MacDougall
26 November 1945

Abstract

This report gives fragment mass distribution data requested by the Bureau of Ordnance for the Navy 3"/50 A.A. projectiles, Mk. 27-3 and Mk. 31-1. Part II (OSRD Report No. 5606) gives similar data for the 3"/50 A.P. projectile, Mk. 29-2. Part III (OSRD Report No. 5608) contains a preliminary investigation of the effect of booster size upon the fragment mass distribution.

The experimental procedure for fragment recovery at this laboratory is described. The fragments are caught in sawdust and recovered by a magnetic separator. Methods of analyzing the data are reviewed. No attempt has been made at this time to examine the physical theory of shell break-up but the results have been described in terms of Mott's semi-empirical exponential distribution law.

Physical tests made upon samples from a single lot, Lot No. 1350 of Mk. 27-3 3" A.A. projectiles showed that the shell were by no means uniform in such properties as

UNCLASSIFIED

UNCLASSIFIED

hardness and tensile strength. It appeared that a simple hardness test could be used to eliminate sub-standard shell without rendering them unfit for use. A set of ten shell selected for uniform hardness did indeed give satisfactorily reproducible fragment mass distribution data when fragmented with cast TNT fillings. At least one additional shell from the same lot but showing subnormal hardness gave a fragment mass distribution significantly coarser than the others.

Composition A was compared with TNT in the Mk.27-3 3" A.A. projectile, but the results were rather sketchy. Down to 1 gram individual mass Composition A gave about 67% more fragments. The effectiveness of these fragments is enhanced by the 20% higher initial velocity.

Tests were made of 50-50 KNO₃/Composition A, a special spotting composition that gives a white burst. The fragment mass distribution in the Mk.27-3 projectile was identical with that of TNT. Tests were made also of an aluminized Composition A. The distribution pattern was intermediate between those of TNT and straight Composition A. There is some indication that the results in this case were influenced by the small size of the projectile and possibly do not represent fairly what aluminized Composition A may do in a large weapon.

The Mk.27-3 projectile was fragmented with TNT-D2 and with Picratol in comparison with TNT. All three explosives gave practically indistinguishable fragment mass distribution patterns.

The Mk.31-1 3" A.A. shell has been fragmented with TNT and with Composition A using both the Mk.58 and the Mk.45 VT fuzes. With the Mk.58 fuze, about 30% of the casing mass comes from the nose surrounding the inert fuze components in the form of 7-9 huge fragments for TNT and 9-11 for Composition A. With the Mk.45 fuze, which is 3/4" longer, 37% of the casing mass is so distributed among 6-7 such massive fragments for TNT and 8-9 for Composition A. The numbers of fragments down to and including about 9 grams individual mass are very slightly greater for Composition A than for TNT, but down to 1 gram, the number for Composition A is about 60% greater than for TNT with the Mk.58 fuze and 47% greater with the Mk.45 fuze, not including the massive nose fragments.

UNCLASSIFIED

UNCLASSIFIED

Studies of Shell Fragment Mass Distribution

Part I - Navy 3"/50 A.A. Projectiles, Mk.27-3 and 31-1

Outline of the Report

	<u>Page</u>
I. Experimental procedure.	4
II. Analysis of fragment mass distribution data.	6
III. Physical properties of the casing.	14
IV. Results.	17
1. Mk.27-3 3"/50 A.A. Projectile.	17
a) Repeated trials with shell of uniform hardness, TNT with Mk. 51 MT fuze.	17
b) Comparison of Composition A with TNT, Mk. 51 MT fuze.	25
c) 50-50 Potassium Nitrate/Composition A and Aluminized Composition A.	30
d) TNT-D2 and Picratol compared with TNT.	34
2. Mk.31-1 3"/50 A.A. Projectile.	42
a) Composition A and TNT with Mk.58 VT fuze.	43
b) Composition A and TNT with Mk.45 VT fuze.	49
c) General summary for Composition A and TNT.	54
Appendix I - Chi-square test for goodness-of-fit of the exponential law.	i
Appendix II - Method of maximum likelihood for fitting the empirical exponential law to the observed fragment mass distribution.	iv

UNCLASSIFIED

UNCLASSIFIED

I. Experimental procedure.

Shell fragmentation at Bruceton has been carried out in a pit 6' in diameter and 6' in depth, having a liner of 3/4" steel. The fragments are caught in sawdust. A diagram of the arrangement is shown in Figure 1. The center of the pit, where the shell is hung, is kept clear by means of a hexagonal box, 15" on edge, constructed of 1/4" plywood or Celotex. The thickness of the sawdust in which the side-wall fragments are caught thus varies between 20" and 22". A 3" shell may expand to more than eight diameters before the side-wall fragments strike the panels retaining the sawdust.

The panels of the box are actually 48" long, but due to the way in which the pit is loaded, the space kept open is only 36" in height. At the bottom of the pit, directly below the location of the shell, several layers of telephone books are placed to stop the faster end fragments. The bottom of the pit is then filled to a depth of 18" with sawdust, including 6" within the box, which is open at the bottom. The box containing the shell is closed on top by a plywood or Celotex panel set within the side panels 18" below the top of the pit. The pit around the box and above the top panel is then completely filled with sawdust. On top of the sawdust, directly over the shell, several more layers of telephone books are placed and the entire pit is then covered over with several layers of sandbags. The sandbags add weight but are practically never reached by fragments.

The original fragmentation pit was inside a reinforced concrete firing chamber used for other studies as well. Observations with typical Navy 3" A.A. shell showed that the shots created negligible disturbance outside the pit, so much of the work was transferred to a second outdoor pit, shown in Plate 1. This facilitated greatly the loading and emptying of the pit while at the same time, the sandbags had sufficient inertia so that further barricading of the pit during shots was unnecessary. We intended ultimately to build a light shelter over the pit to keep out the weather, but operations came to a close before this was accomplished. Meanwhile, during dry weather, the outdoor pit has given extremely satisfactory service.

After the shell has been fired, the sawdust is shoveled into bins and then run through a magnetic separator. The first separator available was a Type M-1 Dings machine, in which the material to be processed passes below a flat disc rotating below the poles of an electromagnet. The steel fragments are picked up on the disc and released as

UNCLASSIFIED

UNCLASSIFIED

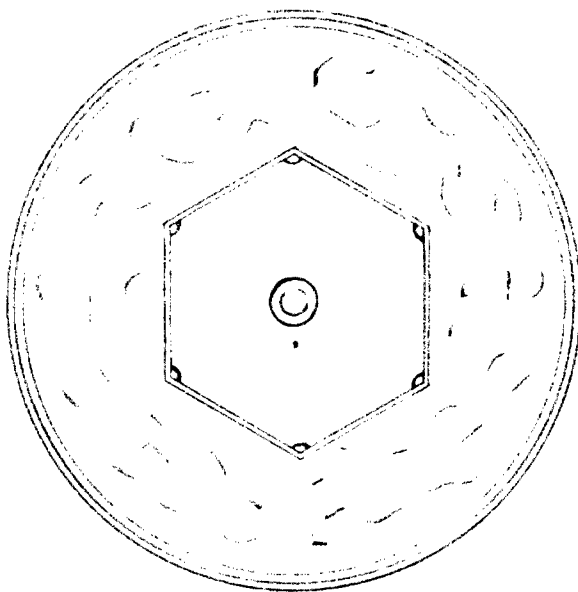
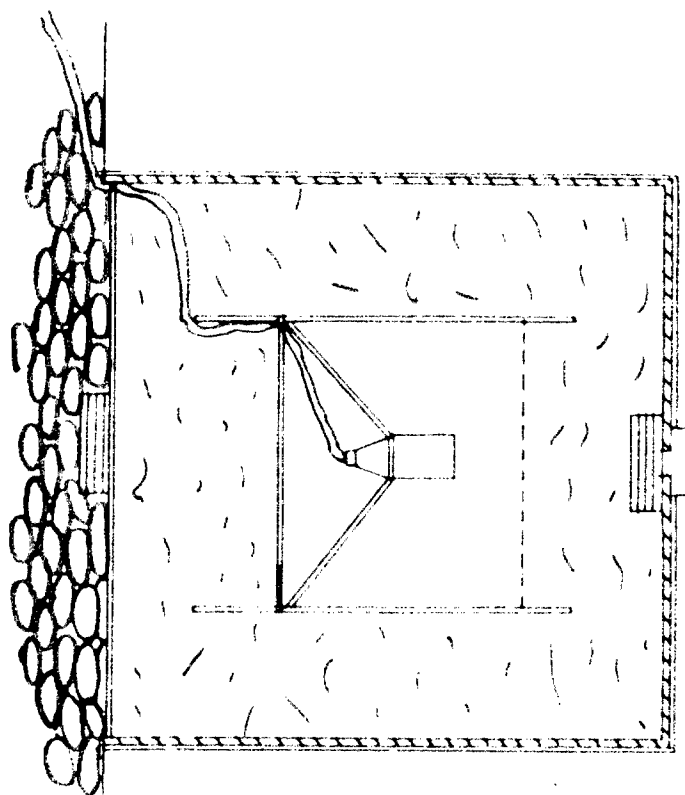


FIGURE 1
DIAGRAM OF FRAGMENTATION PIT LAYOUT
ELEVATION AND PLAN 1" = 2'-0" SCALE

UNCLASSIFIED

UNCLASSIFIED

they are carried out of the magnetic field. This separator effectively recovered steel fragments down to at least 0.25 gram individual weight (the lowest weight in which we were interested) but the operation was quite slow. We have now a Dings Type F-X separator (see Plate 2) in which the sawdust is fed onto a 12" diameter rotating hollow steel drum. A stationary magnet within the drum holds the fragments until they are carried around out of the sawdust stream. This machine is very efficient, picking out everything from the largest steel shell fragments down to extremely fine dust. The operation is rapid so that the entire 180 cubic feet of sawdust used in each shot can be processed easily in about four hours. The sawdust discharged from the separator is passed into storage bins through a screen on which the coarser non-ferrous fragments from the fuze and the rotating band are recovered.

The larger fragments generally have sawdust imbedded in their crevices. This sawdust is removed by heating the fragments at 900°F. for thirty minutes. Such treatment removes more than 90% of the weight of sawdust present, with negligible increase in weight due to oxidation of the steel. The sawdust is removed from the smaller fragments by flotation in carbon tetrachloride, followed by boiling for thirty minutes in 25% sodium hydroxide solution.

After the fragments have been cleaned, it has been our general practice to weigh them individually down to 9 grams weight. The linear dimensions of these fragments have also been taken. These detailed weights and dimensions are available in our original records but in order to save space, they have not been included in this report. Fragments below 9 grams have been sorted into weight groups of from 9 to 4 grams, 4 to 1 gram and 1 to 0.25 gram, counted and weighed collectively in their respective groups. Fragments weighing individually less than 0.25 gram have been grouped together and weighed collectively, but no attempt has been made to count these fragments. This procedure is satisfactory for 3" A.A. and A.P. projectiles, for which at least 95% of the total casing weight consists of fragments weighing individually more than 1 gram. For thinner-walled projectiles giving appreciably finer fragmentation, it would be important to use smaller intervals in grouping the fragments at the fine end of the scale and perhaps even to extend the count to fragments below 0.25 gram individual weight.

UNCLASSIFIED



Plate 1

View of Fragmentation Pit

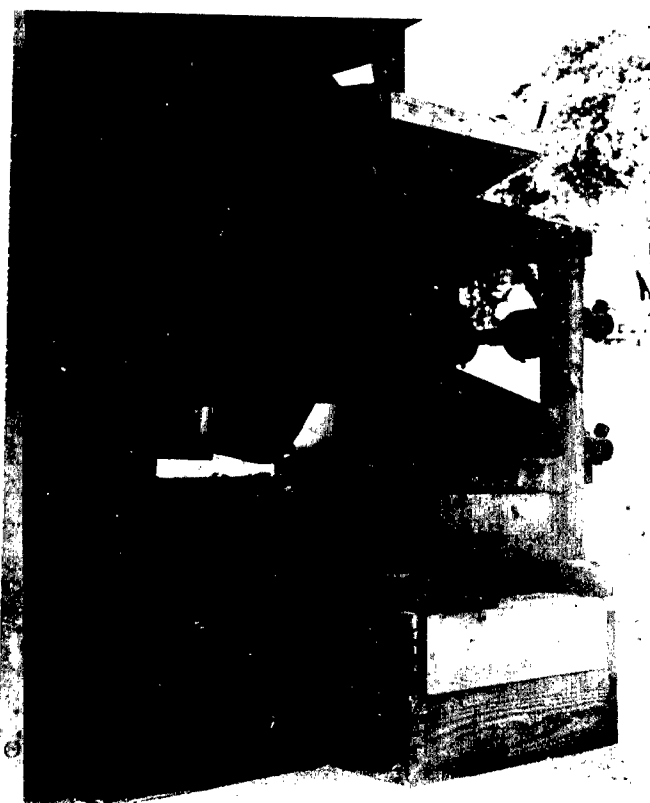


Plate 2

Magnetic Separator,
Dings Type F-X

II. Analysis of fragment mass distribution data

In this report, dealing with the fragmentation of Navy 3" A.A. projectiles, we have been concerned not so much with the general physical theory of shell break-up as with empirical ways to represent the data. For a fundamental theoretical investigation, service projectiles are far from ideal in shape and we should begin such a study by the fragmentation of simple cylindrical tubes.

The fragments from service 3" A.A. and A.P. shell down to individual masses of about 1 gram in many cases, however, satisfy approximately a simple semi-empirical distribution law proposed by N.F. Mott (British Report A.C. 3348, 3642 and a series of subsequent reports). The basic form of this law is:

$$dN = A \exp \left(-\frac{M}{M_0} \right) dM \quad (M = m^{1/2}) \quad (1)$$

where dN is the number of fragments having M (square-root of the individual mass) within the range M to $M + dM$ and where A and M_0 are constants characteristic of the given shell. From (1) we may derive by integration corresponding equations for the number N_{ij} of fragments with masses within the finite range m_i to m_j :

$$N_{ij} = A M_0 (e^{-M_i/M_0} - e^{-M_j/M_0}) \quad (2)$$

and for the cumulative number N_i with masses equal to or exceeding m_i :

$$N_i = A M_0 \exp \left(-\frac{M_i}{M_0} \right) \quad (3)$$

Equation (3) indicates that by plotting $\log N_i$ vs. $M_i (= m_i^{1/2})$, a straight line would be obtained having slope $-0.4343/M_0$. Equation (2) suggests that in sorting the fragments into mass groups, it will be advantageous to take the cuts at limits increasing in proportion to m^2 , e.g., 1 - 4 grams, 4 - 9 grams, 9 - 16 grams, etc. These groups turn out to be of convenient sizes for analyzing the data for typical 3" shell, though of course for larger shell or for thinner-walled casings, a similar principle could be preserved by using a different unit of mass. If the cuts are so taken that always $M_i = i$, $M_j = i+1$, $i = 1, 2, 3, \dots$ Equation (2) reduces to:

$$N_{ij} = A M_0 (1 - e^{-1/M_0}) e^{-i/M_0} \quad (4)$$

Therefore the relation between $\log N_{ij}$ and $M_i (=i)$ under the given convention regarding the size of the mass ranges would also be a straight line with slope $-0.4343/M_0$.

Equations such as (1) and other related types have been discussed also by R. W. Gurney and J. N. Sarmousakis (Ballistic Research Report No. 448) and by W. R. Tomlinson (Picatinny Arsenal Report No. 1404). A law such as (1) is equivalent to that of random break-up in two dimensions. The third dimension of the fragments, the thickness, is quite uniform over all the larger fragments showing both original inner and outer casing surfaces. It is determined by the extent to which the casing expands before rupture. A large fraction of the total mass consists of fragments of this type. The smaller fragments, however, include many produced by rupture in all three dimensions, the relative number increasing as smaller and smaller individual fragment masses are taken into consideration. As may be expected, therefore, one may not properly extrapolate Equations (1) - (4) to include the smallest fragments. The actual numbers of such fragments are larger than the ideal calculated numbers based on the values of A and M_0 that fit the observed distribution of the larger fragments. In practice, for 3" A.A. and A.P. shell, as has been mentioned, Equation (1) apparently fits the data quite well down to fragments having individual masses of about 1 gram. This includes at least 95% of the total casing mass for such shell. While in some cases, fragments as small as 0.25 gram may be individually effective, in general for 3" shell, fragments of less than 1 gram constitute but a small part of the total effectiveness, particularly at a moderate distance from the shell and against all but the lightest targets. Therefore Equation (1) and its derived forms afford a generally satisfactory analytical description of the fragment mass distribution over the useful range of individual fragment masses, provided that we are not interested in the smallest fragments. For thin-walled high-capacity projectiles of similar size, it should be pointed out, fragments of small absolute mass such as 1 gram or even less occur with much greater relative frequencies and high velocities, and they may constitute the bulk of the projectile's effectiveness as a fragmentation weapon. Presumably an equation such as (1) could be fitted to the mass distributions of such projectiles (also to those of projectiles of other sizes) but with a difference in the range of absolute individual fragment masses over which it is valid. Whether this range would include a sufficiently large fraction of the total number of effective fragments for the equation to be useful remains to be examined in each case. The present investigation, however, is concerned exclusively with service 3" A.A. shell.

Mott has pointed out that shell break-up cannot be truly random in two dimensions since there is in general an observed rough correlation between the fragment length and breadth. However, by assuming that fragment dimensions are governed by a primary splitting parallel to the axis into strips, followed by break-up of each strip into segments according to the same law but with the condition that the average length is some fixed multiple of the particular strip's width, he has derived a form of distribution law that when plotted graphically is practically indistinguishable from the simple empirical law represented by Equation (1) (see British Report A.C. 4035). He has also attempted to derive a theoretical expression for M_0 for a given explosive filling in an ideal cylindrical casing, in terms of the rate of casing expansion and the tensile properties of the steel (British Reports A.C. 3642, 4035). According to this theory:

$$M_0 = k t^{1/2} \left(\frac{d}{V}\right)^s \quad (5)$$

where t is the original casing thickness (in.), d the external diameter of the casing (in.), V the initial fragment velocity (ft/sec) and s a constant exponent whose value is about $2/3$. The value of k depends upon the steel and for British and American shell steels, it has the empirical value 176 (fragment masses expressed in grams).

A special complication arises in the case of Navy 3" A.A. shell because of the relatively large space occupied by the fuze and auxiliary detonator and the comparatively short length of the charge. While empirical examination of the fragment mass distribution is useful in itself as a step in the determination of the shell's effectiveness, for theoretical purposes the shell is far from ideal. The booster is buried well within the shell, leaving a rather large fraction of the casing's length towards the nose containing either but a small annular layer of explosive in the case of the MT fuzes or no explosive at all in the case of the VT fuzes. This condition results in the creation of a small number of extremely large nose fragments having velocities well below the average. These fragments naturally do not fit the distribution law satisfied by the others. In the case of the VT fuzes, Mk. 58 and Mk. 45, where the nose fragments have been backed by no explosive at all, it is quite easy to distinguish these fragments from the others since they break off rather sharply at a region corresponding to that at which the explosive filling begins (see Plates 18, 19, 22 and 23). Only when these fragments are excluded from the total do the fragment mass distributions satisfy approximately Equations (1) - (4). We are justified in treating them separately since their demonstrated lower velocities (see OSRD Reports Nos. 5266 and

[REDACTED]

5267 by R. W. Drake) correspond to a different order of effectiveness. In the case of the MT fuze, Mk.51, where the nose fragments have been backed by a thin layer of explosive, the distinction between relatively slow nose fragments and the other side-wall fragments is not so clean-cut. Fragmentation is undoubtedly coarser towards the nose (see Plate 4) but many of the nose fragments, instead of breaking off cleanly in the region of the booster, extend on into the side-wall region below. These nose fragments also have velocities well below the average (OSRD Report No. 5531). For Navy 5" A.A. shell bearing the same fuzes, these complications would presumably not arise since the nose fragments affected by the presence of the fuze would constitute a relatively small fraction of the total casing mass.

One would expect further complications due to the presence of the rotating band and also end-effects at the base of the shell. While the copper rotating band fragments themselves have been segregated from the steel casing fragments, no general attempt has been made to treat the steel base fragments separately from the side-wall fragments, though this would be desirable in a more detailed fundamental investigation.

One may derive physical interpretations of the parameters A and M_0 in Equations (1) - (4) as follows: If the distribution law were valid down to the smallest fragments, it is clear from (3) that the total number would be AM_0 . At the same time, by integrating the expression for $M^2 dN$ in terms of Equation (1), one would obtain for the total mass of the fragments $2AM_0^3$. The average fragment mass would therefore be $2M_0^2$. This provides a tentative physical interpretation for M_0 : if equation (1) were valid over the entire fragment mass range, the square of M_0 would be equal to half the mean fragment mass. An equivalent interpretation may be derived by integrating the expression for $M dN$: we may show then that M_0 would be equal to the mean square-root of the individual fragment mass. The constant A may be eliminated by reference to the total mass of the fragments, W_0 , which is generally known (if recovery is complete, it should be equal to the original casing mass): $A = W_0/2M_0^3$. In Equations (2) - (4), the combination AM_0 could be replaced by $W_0/2M_0^3$. Thus, for a particular shell, with W_0 given, the distribution for a given explosive filling would be characterized by the value of the single parameter M_0 .

Actually, we cannot in practice measure the real total number of fragments nor hence their true average mass, and furthermore, we have noted that Equation (1) is not valid anyhow for the smallest fragments. If it does apply down to some least individual mass m_1 in which we are interested (e.g., 1 gram for

service 3" shell), we may modify the interpretation as follows: Down to individual mass m_1 , the cumulative mass W_1 of the fragments, by integrating the expression for $M^2 dN$, will be

$$W_1 = AM_0 (2M_0^2 + 2M_0 m_1 + m_1^2) \exp \left(-\frac{m_1}{M_0} \right) \quad (6)$$

Since we may readily measure W_1 , Equation (6) together with the value of M_0 serves to fix the value of A , so that just as in the ideal case where $m_1 \rightarrow 0$, the distribution law requires adjustment of only the one parameter M_0 , in addition to the directly observed cumulative mass W_1 , to fit the data. Thus, for the special case $m_1 = 1$ (gram):

$$AM_0 = \frac{W_1 \exp (1/M_0)}{2M_0^2 + 2M_0 + 1} \quad (7)$$

By integrating the expression for $M dN$, we may show furthermore that:

$$M_0 = \overline{m^{1/2}} - (m_1)^{1/2} \quad (8)$$

where the average represented by the first term on the right is taken only over those fragments with masses equal to or exceeding m_1 . In other words, so long as Equation (1) accurately represents the distribution for all those fragments with individual masses equal to or exceeding m_1 , M_0 accurately represents the excess of the mean square-root of their fragment mass over the square-root of the limit mass m_1 . Of course in the ideal case discussed previously where m_1 can be taken as zero, Equation (8) reduces to $M_0 = \overline{m^{1/2}}$ averaged over all the fragments.

Equation (8) constitutes the most straightforward method of calculating M_0 from the observed data for a given shell, though it is a tedious one since it involves taking the square-root of each individual mass before averaging. By comparing (6) with (3) however, we may derive an equivalent expression for M_0 in terms of the mean fragment mass, $\bar{m} = W_1/N_1$, averaged over all the fragments of interest having individual masses equal to or exceeding m_1 :

$$\bar{m} = 2M_0^2 + 2M_0 m_1 + m_1^2 \quad (9)$$

$$\therefore M_0 = \frac{(2\bar{m} - m_1)^{1/2} - (m_1)^{1/2}}{2} \quad (10)$$

For the special case $m_1 = 1$ (gram):

$$M_0 = \frac{\sqrt{2\bar{m} - 1} - 1}{2} \quad (11)$$

One should note that if Equation (11) is used to calculate M_0 and Equation (7) to calculate AM_0 (and by inference A), one is in fact adjusting A so that Equation (3) is exactly satisfied by the observed data for $M_1 = 1$, $N_1 = N_1(\text{observed})$. This becomes evident upon substitution of (9) with $M_1 = 1$ in (7), observing that by definition $\bar{m} = W_1/N_1$, and comparing with (3). Therefore we could equally well use Equation (3) in the form:

$$AM_0 = N_1 \exp \left(\frac{1}{M_0} \right) \quad (11')$$

to fix AM_0 from the observed value of N_1 and the computed value of M_0 according to (11).

We may determine a value of M_0 by using a more elegant statistical approach, the method of maximum likelihood. By this method, suggested to us informally by Dr. L. H. Thomas of the Ballistic Research Laboratory, a value of M_0 is selected that makes the observed fragment mass distribution most probable, assuming that it tends to follow the exponential law (1), as compared with all other possible values of M_0 . The procedure, which takes no explicit account of the cumulative fragment mass, is outlined in Appendix II. It has the theoretical advantage of taking greater account of the actual distribution in detail instead of assigning M_0 on the basis merely of an averaged mass. On the other hand, for the shell that we have analyzed by both methods, the difference in the estimated values of M_0 has been less than 5%, or no greater than the variation in M_0 from shot to shot in a series of repeated shots. We have preferred to use (11) to estimate the value of M_0 because the equation is so simple to apply. It involves the assumption that the actual distribution does in fact satisfy rather accurately the empirical equation (1), but if this is not so, the value of M_0 obtained by any statistical method has little significance.

By Equation (11), we can always calculate formally a value of M_0 for any given distribution, whether or not the distribution fits Equation (1). To show whether Equation (1) does indeed fit the data, allowing for random statistical fluctuations, we may apply the Chi-square test, as suggested to us by Dr. H. Scheffe of the Applied Mathematics Panel. This test is described in Appendix I and shows whether at a given level of confidence the data are consistent with the assumed law or whether this assumption must be ruled out as too unlikely.

A different form of fragment distribution law has been proposed by W. Payman (British Report A.C. 4604). This law describes empirically the fraction W_1/W_0 of the total casing mass accumulated in fragments having individual masses equal to or

exceeding m_i , as a function of m_i :

$$\log W_i/W_0 = -c m_i \quad (12)$$

Obviously Equations (12) and (1) cannot be exactly consistent with each other. If we were to assume that (1) is applicable over the entire distribution down to and including the smallest fragments, so that AM_0 in Equation (6) could be replaced by $W_0/2M_0^2$, we should obtain as the expression equivalent to (12):

$$\log W_i/W_0 = -0.4343 \frac{M_i}{M_0} + \log \left(1 + \frac{M_i}{M_0} + \frac{M_i^2}{2M_0^2} \right) \quad (13)$$

Actually, the assumption is in this case a not unreasonable one since even though the numbers of very small fragments (i.e. smaller than 1 gram) do in fact depart widely from those that would be calculated in accordance with Equation (1), their contribution to the total mass is relatively small, e.g., less than 5%, so that substitution of a calculated instead of the observed contribution to the cumulative mass over this range can introduce no appreciable error. For (12) and (13) to be consistent with each other, it readily follows that:

$$c M_0^2 = \frac{0.4343}{M_i/M_0} - \frac{1}{(M_i/M_0)^2} \log \left(1 + \frac{M_i}{M_0} + \frac{M_i^2}{2M_0^2} \right) \quad (14)$$

The expression on the right of Equation (14) has been computed for various assumed values of M_i/M_0 , as follows:

M_i/M_0	W_i/W_0	$c M_0^2$
4.0	0.238	0.0390
3.5	0.321	0.0403
3.0	0.423	0.0415
2.5	0.544	0.0423
2.0	0.677	0.0431
1.5	0.809	0.0410
1.0	0.920	0.0364

One sees that over the range of W_i/W_0 between about 0.30 and 0.85, cM_0^2 is nearly constant with a value between 0.040 and 0.043. T. H. Wise has shown from experimental results with various shell that a constant value of cM_0^2 averaging about 0.0412 is in fact

obtained (A.R.D. Theoretical Research Report 23/44). He has suggested using an equation such as (13) to calculate M_0 from observed cumulative fragment mass data. A further review of this treatment is given by N. F. Mott, J. H. Wilkinson and T. H. Wise in A.R.D. Theoretical Research Report 37/44.

The near constancy of cM_0^2 in the range of W_i/W_0 between 0.30 and 0.85 implies that if Mott's equation, Equation (1), fits the observed fragment mass distribution over that range, then, Payman's equation, Equation (12) approximately will also. Conversely, if Equation (12) fits the observed data, then over the range W_i/W_0 between 0.30 and 0.85, Equation (1) will fit it also, with a value of M_0 approximately equal to $0.0415/c$. Beyond 0.85, Equation (12) will be rather insensitive to the fragment mass distribution in terms of numbers, so the fact that Equation (12) may be valid over that range (that of the smallest fragments) suggests nothing specific about the actual mass distribution in terms of numbers. We have stated that for many shell, Equation (1) continues to be valid down to W_i/W_0 of about 0.95, beyond which it no longer fits the data. While such behavior may be technically inconsistent with application of Equation (12) in that range (i.e. beyond 0.85), in practice Equation (12) could still continue to be approximately satisfied without implying anything precise about the numerical distribution. In the range of W_i/W_0 below 0.30, Equations (1) and (12) become increasingly incompatible with each other as W_i/W_0 is taken smaller and smaller. However, this range includes only a few of the largest fragments and one would be inclined for practical purposes to discount departure of the observed distribution from either (1) or (12) if these equations were found to fit the data with reasonable accuracy over the middle range of W_i/W_0 .

Whether Equation (1) with its derived forms, (2) and (3), or Equation (12) is the more useful analytical formulation depends upon the particular application. In general, we favor (1) and particularly (3) giving the cumulative number as a function of the individual fragment mass. The reason is that since the fragments from a conventional shell are distributed over a fairly narrow range of velocities, there will be some rather well-defined lower critical mass for a given target such that all heavier fragments have a reasonable expectation of penetrating through it (in a precise treatment the additional factors of retardation and orientation to the target must of course be taken into consideration). If this critical mass has been determined, Equation (3) then gives directly the number of effective fragments. On the other hand, an equation such as (12) may be the more useful in the study of controlled fragmentation, where we may be interested in efficiently transforming a large fraction of the total casing mass into fragments of a predetermined size.

III. Physical properties of the casing.

The non-uniform behavior of shell in pit fragmentation studies has been commented upon (R. W. Gurney and J. N. Sarmousakis - Ballistic Research Laboratory Report No. 448). Considerable variation in the numbers of fragments has been noted even from members of a single lot of shell, though Picatinny Arsenal claims to have improved the reproducibility greatly by careful control over the method of initiation (P.A. Report No. 1530 by G. M. Hopkins). Variations in the quality of the casing as well as the possible presence of small scratches on the surfaces have no effect upon the fragment velocities, which for a given explosive are governed solely by the charge weight/casing weight ratio (except for end effects), but they may have a very large effect upon the numbers of fragments produced.

The fact that the elementary precaution of selecting the shell for an experimental investigation from a single lot affords insufficient protection against drawing unrepresentative samples was brought home to us by physical tests run on six shell taken at random from a lot of five-hundred Mk.27-3 3" A.A. shell, Lot No. 1350, sent to us from the Naval Ammunition Depot, Fort Mifflin. The sample shell were given to the Pittsburgh Testing Laboratory for examination. Each was quartered longitudinally and test specimens were taken from each of the four quarters. The test results are given in condensed form in Table I.

Table I

Physical Tests of Mk.27-3 3" A.A. Shell
Drawn From Lot No. 1350

<u>Shell</u>	<u>Sample</u>	<u>Yield Strength (psi.)</u>	<u>Tensile Strength (psi.)</u>	<u>Elongation (%)</u>	<u>Brinell Hardness</u>
1	A	106,520	124,220	30.0	255
	B	103,700	123,280	24.3	255
	C	105,980	123,430	24.3	262
	D	109,050	123,010	21.4	255
2	A	100,900	122,580	24.3	255
	B	101,100	122,900	24.3	269
	C	107,550	122,100	22.9	262
	D	104,620	123,520	22.9	262
3	A	61,430	77,640	25.7	217
	B	82,020	109,600	24.3	229
	C	87,440	108,850	25.7	229
	D	90,460	109,550	23.6	229
4	A	96,900	115,700	25.7	241
	B	101,420	115,850	25.7	241
	C	97,490	115,890	22.9	241
	D	99,500	115,800	25.7	241
5	A	92,900	118,290	25.7	241
	B	95,480	117,300	24.3	248
	C	92,970	117,100	24.3	248
	D	97,000	116,490	22.9	248
6	A	101,800	115,700	24.3	248
	B	100,000	116,400	25.7	241
	C	101,500	115,100	25.7	241
	D	95,900	114,700	25.7	241

[REDACTED]

One sees that of the six shell, one, No. 3, was well below the others in quality and actually failed to meet specifications. Shell Nos. 4, 5 and 6, while greatly superior to No. 3, were still inferior to Nos. 1 and 2, though we do not know how a difference of this order of magnitude would affect shell break-up. Fortunately there appears to be a correlation between the hardness, which can be measured without destroying the individual shell, and the yield and tensile strengths. This correlation can be used in at least a negative sense to reject substandard shell showing abnormally low hardnesses, even though it will be impossible to measure the actual strengths of the shell accepted for investigation on the basis of this test. As shown in the following section, ten more shell from this lot, accepted on the basis of uniform hardness results, were loaded with cast TNT and fragmented. The average number of fragments down to 1 gram individual mass was 285 with standard deviation of 19, showing a quite acceptable degree of consistency. On the other hand, at least one additional shell from the same lot, whose hardness was well below the average for the ten, gave a significantly coarser fragment mass distribution, the number of fragments down to 1 gram being only 244.

We may conclude that for a precise study of fragment mass distribution, not only should the shell all be selected from the same lot but in addition, individual hardness measurements should be taken and used as a basis for further selection. If this is not done, one runs the risk of obtaining inconsistent results whose interpretation is obscured by undetected differences in the quality of the individual casings. Furthermore, one should take care to avoid surface scratches since a scratch only 0.004" deep has been shown to favor fracture along the scratch in preference to other neighboring locations (see British Report A.C. 1241 by H. L. Porter).

IV. Results.

1. Mk.27-3 3"/50 A.A. Projectile.

a) Repeated trials with shell of uniform hardness, TNT with Mk.51 MT fuze.

A set of ten Mk.27-3 3" projectiles was selected from Lot No. 1350 on the basis of uniform hardness. The average hardness ranged between 25.7 and 27.5 on the Rockwell C scale. In addition, two shell with lower average hardnesses, 19.7 and 21.1, respectively, were selected from the same lot. These shell were loaded with cast TNT and drilled out to receive the service Mk.51 mechanical time fuze and Mk.54 auxiliary detonator. The fuzes were dummies with the clock-work replaced by a brass plug of equal weight. The auxiliary detonator, armed for static firing, was initiated by means of a No. 8 duPont electric blasting cap inserted on the axis of the fuze and butting against the firing-pin of the auxiliary detonator. The empty casing weights, without fuzes, averaged 4118 ± 8 g. and the main charge weights averaged 363 ± 3 g., the density being about 1.60. The auxiliary detonators contained the standard 15 g. Tetryl boosters.

The object of these shots was to obtain statistical information on the reproducibility of the fragment mass distribution when care had been taken to eliminate variations in casing hardness (and presumably along with it, variations in other physical properties of the steel).

The results are summarized in Table II. The fragments from a typical shell are shown arranged according to mass in Plate 3. The same fragments are shown in Plate 4 arranged approximately according to the region of the shell from which they came. In Plate 4, no attempt has been made to locate fragments having masses of less than 1 gram. The smaller fragments have merely been grouped in the piles shown at the top of the picture. The thickness of typical side-wall fragments ranged between 0.35" and 0.40", the average being about 0.37". The original casing thickness was 0.54".

Table II includes values of M_0 and AM_0 , calculated for each shell in accordance with Equations (11) and (11') and also the value of $\sum x^2$ calculated as shown in Appendix I.

Table II

Mk. 27-3 3" A.A. Projectile, TNT-loaded, Mk. 51 MT Fuze and Mk. 54 Auxiliary Detonator

Initial data:	#70	#71	#73	#74	#75	#76	#77	#78	#79	#80	#81	#98
			(All weights in grams)									
Casing hardness, Rockwell C	26.9	27.0	26.5	26.5	27.5	26.6	25.7	26.8	26.6	27.3	19.7	21.1
Total weight, loaded shell	4485	4470	4481	4489	4481	4482	4484	4481	4483	4463	4490	4495
without fuze or adapter	364	369	368	361	356	361	361	363	364	364	359	367
Charge weight	4121	4101	4113	4128	4125	4121	4123	4118	4119	4099	4131	4128
Casing weight	204	204	204	204	204	204	204	204	204	204	204	204
Copper rotating band**	3917	3897	3909	3924	3921	3917	3919	3914	3915	3895	3927	3924
Casing steel	357	357	358	356	358	356	357	356	356	356	356	356
Fuze adapter	343	338	337	337	344	335	337	338	337	338	336	345
Mk. 54 auxiliary detonator	15	15	15	15	15	15	15	15	15	15	15	15
Booster weight	658	651	653	658	654	656	652	658	654	651	656	654
Mk. 51 fuze												
Metal parts, fuze+aux. det. +adapter	1343	1331	1333	1336	1341	1332	1331	1337	1332	1330	1333	1340

General recovery data:

Casing steel fragments***	(4715)*	4068	4050	3980	3951	3931	4008	3938	3933	3922	3965	3952
Weight of all fragments	3792	3756	3788	3799	3767	3773	3841	3753	3789	3755	3824	3822
1 gram												
Copper fragments from rotating band	200	204	189	200	202	199	200	208	198	195	201	198
Fragments from fuze, aux. det. and adapter	1326	1305	1311	1299	1308	1326	1324	1332	1326	1308	1315	1318

*This shot was the first on which the new separator was used. The steel recovered included a quantity of extremely fine dust (669 grams finer than 20-mesh compared with only about 30 grams in this range for later shots) evidently accumulated from previous shots. This has no effect on the numbers of fragments down to 0.25 grams.

**Nominal weight. Casing steel weight may be in error by several grams due to possible small variations in this quantity.

***May include a small quantity of fragments from fuze, auxiliary detonator or adapter, not identifiable as such.

Table II (Continued)

	#70	#71	#73	#74	#75	#76	#77	#78	#79	#80	#81	#98
<u>Detailed recovery data:</u>												
<u>Casing steel fragments</u>												
No. with mass > 225 grams												
196	0	0		1	0	0	0		0	0	0	0
169	1	1		2	1	1	2		1	0	1	1
144	1	1		2	1	1	3	0	1	4	2	2
121	3	1	0	4	1	2	3	0	1	4	5	6
100	3	4	3	4	3	4	5	3	5	6	8	9
81	4	7	9	7	9	8	10	5	8	7	9	9
64	9	10	10	11	13	10	13	9	12	10	14	9
49	17	17	15	21	19	16	19	17	17	14	22	13
36	24	23	26	24	25	23	22	23	22	20	26	21
25	32	37	34	32	35	32	32	30	37	28	36	40
16	61	67	61	57	55	65	59	54	58	55	59	65
9	124	116	114	109	108	127	111	121	104	118	110	116
4	178	167	178	161	176	176	167	194	172	199	157	171
1	301	269	292	268	284	272	260	315	279	308	244	269
0.25	433	431	418	383	444	413	394	490	404	472	370	400
<u>Average mass of fragments with individual mass > 1 gram</u>												
	12.60	13.96	12.97	14.18	13.26	13.87	14.77	11.91	13.58	12.19	15.67	14.21
M _O	1.96	2.09	2.00	2.12	2.03	2.09	2.17	1.89	2.06	1.92	2.25	2.12
AM _O	501	434	482	430	466	439	413	535	454	519	380	432
2*	19.67	9.16	7.13	15.86	11.13	23.05	12.67	12.21	4.03	16.41	14.16	6.80
*For significance see Appendix I.												
<u>Copper rotating band fragments</u>												
No. with mass between 0.10 and 16 grams**	47	42	55	42	44	47	67	68	72	56	45	75
**Average mass of heaviest fragment = 10.2 g.												
<u>Fuze, aux. det. and adapter fragments</u>												
No. with mass > 100 grams	3	4	3	5	3	3	3	3	3	3	3	4
" " 49-100 "	2	1	1	0	0	0	0	0	1	0	0	0
" " 9-49 "	3	6	6	6	6	5	4	2	9	4	7	6
" " 0.1-9 "	47	58	53	47	54	83	78	102	115	57	65	34

In Table III are summarized the estimated average cumulative numbers of steel casing fragments, with their estimated standard deviations for the ten uniform shell, Nos. 70, 71, 73-80. These averaged data are plotted graphically in Figure 2. The table includes also values calculated according to the empirical equation:

$$N_i = 466 \exp \left(- \frac{M_i}{2.03} \right)$$

where 2.03 with estimated standard deviation 0.09 is the estimated average value of M_0 and 466 is the value of AM_0 that with this value of M_0 gives correctly the observed average value 285 of N_i . The straight line in Figure 2 has been drawn to correspond with this equation.

Table III

Average cumulative numbers of steel casing fragments with individual masses equal to or exceeding m_i , Mk.27-3 3" projectile, TNT, with Mk.51 MT fuze.

m_i (grams)	Average N_i obs.	Std. deviation	N_i (empirical equation)	Difference, obs. - calc.
100	4	1	3	+ 1
81	7	2	6	+ 1
64	11	2.5	9	+ 2
49	17	2	15	+ 2
36	23	2	24	- 1
25	33	3	40	- 7
16	59	4	65	- 6
9	115	7	106	+ 9
4	177	4	174	+ 3
1	285	19	(285)	(0)
0.25	428	34	364	+ 62

Upon examining the observed results, one sees that the data for the ten shell are reasonably consistent, particularly down to individual fragment masses of at least 1 gram. Even down to 0.25 gram, the greatest individual departure from the average number is less than 15% of the average.

The data for Shell No. 81, which had a subnormal hardness, show a definitely coarser distribution pattern. The number of fragments down to and including 1 gram individual fragment mass, for example, is smaller than the average for the

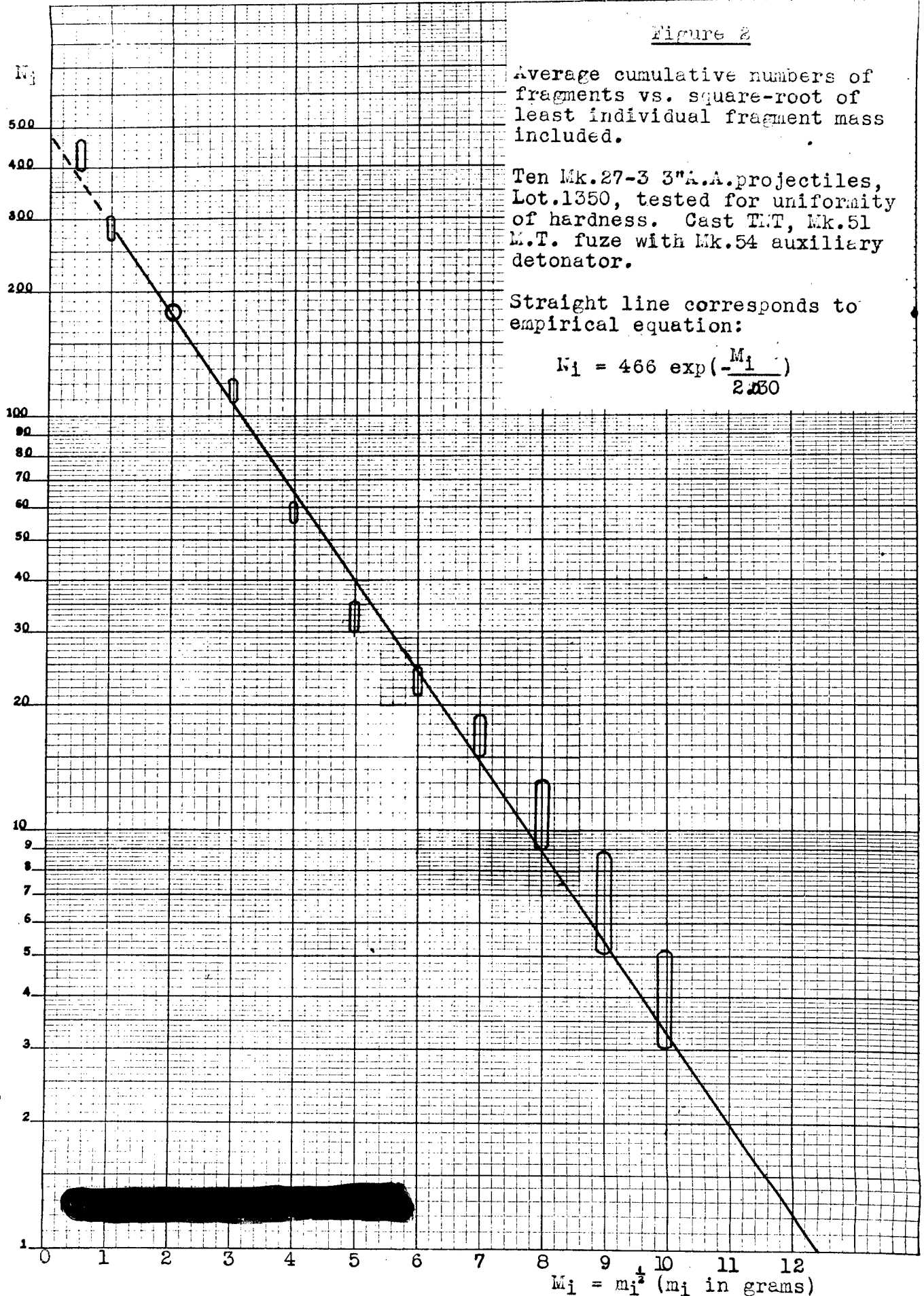
Figure 2

Average cumulative numbers of fragments vs. square-root of least individual fragment mass included.

Ten Mk.27-3 3"A.A.projectiles, Lot.1350, tested for uniformity of hardness. Cast T.M.T, Mk.51 M.T. fuze with Mk.54 auxiliary detonator.

Straight line corresponds to empirical equation:

$$N_1 = 466 \exp\left(-\frac{M_1}{2.530}\right)$$



preceding ten shell by more than twice the standard deviation, indicating that at a confidence level of 95%, this shell is distinguished from the others. For Shell No. 98, whose hardness was not quite as low as that of No. 81, though well below the average for the ten uniform shell, the fragmentation was coarser than the average but not sufficiently so to distinguish this shell from the others. It falls among the three coarsest distributions in the series of ten.

According to the Chi-square test for goodness of fit of empirical Equation (1), six of the twelve shell, Nos. 71, 72, 75, 78, 79 and 98 may be regarded as having distributions that are not inconsistent with the equation; for four, Nos. 74, 77, 80 and 81, the hypothesis is rejected at significance level of 5% but not at 1%; for two, Nos. 70 and 76, the hypothesis is rejected at level 1%. Rejection implies that the departures from the law in individual fragment mass categories are too large to be supposed consistent with merely random statistical fluctuations. All of the shell show a systematic departure from the exponential law in the range 9-16 grams; the observed number in this range (average = 56 for the ten uniform shell) is in every case greater by an amount varying from 5 to 22 than the number consistent with the empirical equation. All but No. 98 show likewise a small departure in the opposite direction in the range between 25 and 36 grams, the observed numbers (average = 10 for the ten uniform shell) being smaller than the numbers consistent with the empirical equation by amounts varying from 1 to 9. These departures contribute heavily to the rejections indicated by the Chi-square test. Nevertheless, since no other simple empirical equation fits the data any better, we have averaged M_0 and AM_0 for the ten uniform shell (one notes that these quantities for Shell No. 81 likewise differ from the averages by more than twice the standard deviations) and tabulated the values of N_i computed according to Equation (3) in Table III. Except between 36 and 9 grams, the fit is excellent down to 1 gram, the differences between the observed and the calculated values of N_i being nowhere greater than the standard deviations of the observed values. Below 1 gram, as previously noted, the empirical equation fails altogether, the actual numbers of fragments in this range greatly exceeding the numbers consistent with the equation.

We have attempted to analyze in greater detail the nature of the fragment mass distribution in the range 9-36 grams. For the Mk.27-3 shell, it is quite easy to identify the

[REDACTED]

origins of all the larger fragments (e.g., generally down to 1 gram) because of the presence or absence of various characteristic surface features such as nose adapter threads, rotating band seat, base crimps for the propellant case, etc. (see Plate 4). The shape is in fact far from that of an ideal cylindrical casing, though the explosive cavity itself is practically cylindrical over almost its entire length. In Table IV we have sorted out within various mass ranges down to 1 gram all the fragments from three representative shell (#70, 75 and 79) approximately according to the part of the casing from which they came. There is naturally a certain amount of overlapping in defining such regions of origin since some larger fragments include more than one region, and furthermore there is uncertainty in determining the origins of some of the smaller fragments, but in general, the fragments are readily classified.

Table IV

Classification of fragments according to origin,
Mk.27-3 3" A.A. projectile, Mk.51 MT fuze

Numbers of fragments						
Mass range (g.)	Showing nose adapter threads	From central side-wall, down to rotating band	From under rotating band	From side-wall, base to rotating band	From base	Total
<u>Shell No. 70</u>						
> 100	0	3	0	0	0	3
81 - 100	0	1	0	0	0	1
64 - 81	0	5	0	0	0	5
49 - 64	0	7	0	0	1	8
36 - 49	0	7	0	0	0	7
25 - 36	0	6	0	1	1	8
16 - 25	5	13	1	7	3	29
9 - 16	5	16	12	24	6	63
1 - 9	5	128	20	20	4	177
Total > 1 gram:	15	186	33	52	15	301
<u>Shell No. 75</u>						
> 100	0	3	0	0	0	3
81 - 100	0	6	0	0	0	6
64 - 81	0	4	0	0	0	4
49 - 64	0	5	0	0	1	6
36 - 49	0	5	0	0	1	6
25 - 36	0	6	0	3	1	10
16 - 25	2	11	1	1	5	20
9 - 16	10	12	15	13	3	53
1 - 9	2	110	27	35	2	176
Total > 1 gram:	14	162	43	52	13	284
<u>Shell No. 79</u>						
> 100	0	5	0	0	0	5
81 - 100	0	3	0	0	0	3
64 - 81	0	4	0	0	0	4
49 - 64	0	4	0	0	1	5
36 - 49	0	5	0	0	0	5
25 - 36	0	12	0	1	2	15
16 - 25	1	12	1	3	4	21
9 - 16	7	4	8	24	4	46
1 - 9	4	104	38	25	4	175
Total > 1 gram:	12	153	46	53	15	279

[REDACTED]

One sees that a characteristic feature of the mass range between 9 and 16 grams is a large influx of fragments from the base and base side-wall, beyond the end of the explosive cavity. This type of fragment appears also in the range between 1 and 9 grams but their relative effect there upon the total number is small because of the large number of true side-wall fragments appearing in this range. The apparently better agreement of the fragments from Shell No. 79 with the exponential law in the range 9-16 grams (reflected also in the unusually low value of $\bar{x} \approx 2$) is due to the abnormally low number of true side-wall fragments (including fragments from under the rotating band) for this shell in this range, so that the base side-wall fragments have the effect of compensating for the deficiency of true side-wall fragments instead of markedly increasing the total number as they do in the cases of the other shell. The reason for such a variation in the detailed distribution pattern obviously cannot be detected without further experimental study.

Clearly, a fundamental study of shell break-up should begin with long cylindrical casings, having perhaps extensions of a different metal such as brass to reduce end effects in the main steel central portion. The simple exponential law (1) or (3) meanwhile remains a useful analytical way of representing the data with fair accuracy even for actual shell, though its limitations should be recognized.

The investigation that has been described in this section has served primarily to demonstrate that reasonably uniform fragmentation data can be obtained by ensuring uniform hardness in addition to selecting the samples from a uniform lot. Even within a given lot of shell, individual variations in mechanical properties may occur that can result in significantly different fragment mass distributions.

b) Comparison of Composition A with TNT, Mk. 51 MT fuze

In addition to the shell described in the preceding section, we have fragmented four Mk. 27-3 3" projectiles, two containing the standard service loading of 0.75 lb. cast TNT and two containing experimental loadings of 370 grams pressed Composition A-3. The shell were service-loaded and were from different lots, without hardness tests, so the exact significance of the results must be discounted accordingly. The two TNT-loaded shell (Shots #18 and 21) bore Lot Number 1642-1937 and were received from NAD, Fort Mifflin, while the two Composition A-loaded shell were Lot Numbers 161-1937 (Shot No. 19) and 194-1937 (Shot No. 23) and were received from NAD, St. Julien's Creek.

The shell were initiated with Mk. 51-2 mechanical time fuzes and Mk. 46 auxiliary detonators. The detonators were armed by removing the centrifugal detents from the firing pins and turning the rotors to the armed position. The fuzes were modified for static initiation by drilling a small hole through the side into the primer cavity below the striker pin and inserting an electric match-head in place of the primer. The match-head ignited the powder ring of the fuze, thus generating pressure in the normal way to drive in the firing pin of the auxiliary detonator. The clock-work of the fuze was present but was of course not in action.

The fragmentation data for these shell are presented in Table V. Plates 5 and 6 show the fragments for one of the TNT-loaded and for one of the Composition A-loaded shell with the steel casing fragments arranged in order of decreasing mass. Plates 7 and 8 show the same fragments arranged respectively according to the approximate parts of the casings from which they came. (Note that the fuze cavity was as shown in Plate 4.)

The Mk. 51 mechanical time fuze contains about 72 grams of steel and 518 grams of non-ferrous metal parts, while the Mk. 46 auxiliary detonator contains 220 grams of steel and 106 grams of non-ferrous metal parts. Most of the steel parts from these components are quite characteristic and readily differentiated from steel fragments coming from the casing proper. The smaller fragments are less readily identified and it is possible that a few have been included among the casing fragments. This would account for minor discrepancies in Table V, particularly the apparently high recoveries of steel casing fragments in Shots #18 and 23. The overall metal recoveries in Shots #18 and 21 were respectively 15 and 8 grams high. Part of the differences may be due to small departures of the actual charge weights from the nominal value of 0.75 lb. specified by the Bureau of Ordnance. We could not measure the charge weights directly, since the shell were received already loaded. In Shots #19 and 23, the total metal recoveries were 108 and 41 grams low respectively out of original totals of about 5400 grams. Most of the losses were in non-ferrous parts (more difficult to recover) of the fuzes and auxiliary detonators, both of which were noticeably more battered for these Composition A-loaded shell than for the TNT-loaded shell.

Table V

Mk. 27-3 3" A.M. Projectile, TNT and Composition A-3,
Mk. 51-2 MT Fuze and Mk. 46 Auxiliary Detonator

<u>Initial data:</u>	<u>TNT</u>		<u>Composition A-3</u>	
	<u>#18</u>	<u>#21</u>	<u>#19</u>	<u>#23</u>
Total weight, loaded shell without fuze or adapter	4484 g.	4469 g.	4478 g.	4491 g.
Charge weight*	340	340	370	370
Casing weight	4144	4129	4108	4121
Copper rotating band**	204	204	204	204
Casing steel	3940	3925	3904	3917
Fuze adapter	356	358	352	357
Mk. 46 auxiliary detonator	342	346	342	341
Booster weight	15	15	15	15
Mk. 51-2 fuze	603	605	609	604
Metal parts, fuze + aux. det. + adapter	1282	1290	1284	1283
<u>General recovery data:</u>				
Casing steel fragments***	3977	3925	3906	3945
Weight of all fragments >1 gram	3819	3754	3658	3728
Copper fragments from rotating band	198	204	191	190
Adapter parts		356	351	358
Aux. det. parts	} 717	318	261	284
Fuze parts	549	623	574	586

*Nominal values, as specified by the Bureau of Ordnance.
Derived casing weights may be in error by several grams,
due to variations in these quantities.

**Nominal value. Casing steel weights may be in error by
several grams, due to variations in this quantity.

***May include small fragments from fuze and auxiliary deton-
ator not identifiable as such.

Table V (continued)

	<u>TNT</u>		<u>Composition A-3</u>	
	<u>#18</u>	<u>#21</u>	<u>#19</u>	<u>#23</u>
<u>Detailed recovery data:</u>				
<u>Casing steel fragments</u>				
No. with mass > 169 grams	1	1		
144	2	2		
121	2	3		0
100	4	5		1
81	7	10		1
64	15	14	0	2
49	18	18	8	11
36	23	23	20	23
25	38	32	37	37
16	61	65	65	58
9	107	103	129	106
4	156	166	209	228
1	252	254	430	413
0.25	380	384	706	576
<u>Average mass of fragments</u>				
with individual mass > 1 gram	15.16	14.78	8.51	9.03
M_o	2.21	2.17	1.50	1.56
AM_o	396	402	837	782
Σx^2	9.92	11.25	(13.30)*	(9.83)*
*See Appendix I for significance. Values for Shots ## 19 and 23 were calculated for five degrees of freedom instead of the usual six.				
<u>Copper rotating band fragments</u>				
No. with mass between:				
9 and 12 grams	2	4	0	0
0.25 and 9 grams	58	35	76	90
<u>Fuze, aux. det. and adapter fragments</u>				
No. with mass:				
greater than 100 grams	3	4	3	4
between 49 and 100 grams	1	1	3	4
between 9 and 49 grams	1	6	14	12
between 0.25 and 9 grams	29	16	105	195

[REDACTED]

The data for the two TNT-loaded shell are in excellent agreement with each other, though the fragmentation is definitely a little coarser than for the ten shell described in the preceding section. It rather closely resembles that of Shell No. 81. The distributions are described quite well down to 1 gram individual fragment mass by the empirical exponential law:

$$N_i = 339 \exp \left(- \frac{M_i}{2.19} \right)$$

(see Figure 3). The data for the two Composition A-loaded shell are less consistent with each other. Shell No. 23 has a distribution consistent with the exponential law but for Shell No. 19, the Chi-square test rejects this hypothesis at significance level of 5%, though not at 1%. Shell No. 19 gave no casing fragments more massive than 64 grams, and gave many more extremely small fragments (e.g., 0.25 - 1 gram) than did Shell No. 23. One should note that these shell were from different lots. The data for the two shell are plotted in Figure 4, together with the straight line corresponding to the empirical equation:

$$N_i = 805 \exp \left(- \frac{M_i}{1.53} \right)$$

We are not justified in drawing definitive conclusions on the basis of so few shots, particularly in view of the absence of information concerning the quality of the particular shell. However, the results do indicate that if we are interested in fragments with individual masses down to less than about 13 grams, Composition A is superior to TNT in numbers of fragments produced. Down to 1 gram individual mass, for example, the number produced by Composition A is about 67% greater than the number produced by TNT. The effectiveness of Composition A is further enhanced by the higher fragment velocity, averaging 2530 ft/sec. at 9' from the shell as compared with an average of 2060 ft/sec. for TNT (OSRD Report #5531 by R. W. Drake).

It is interesting to compare N. F. Mott's theoretical formula (5) for M_0 with the observed values. The original casing thickness of the FK. 27-3 3" projectile is 0.54" over most of its length. Putting this value in Equation (5) together with the velocities just quoted, we obtain theoretical M_0 values of 1.65 for TNT and 1.44 for Composition A. The calculated value for Composition A is in fair agreement with the observed value. For TNT, however, the observed distribution is considerably coarser than that corresponding to the theoretically calculated value of M_0 . Part of the discrepancy is undoubtedly due to the coarse fragmentation of the upper half of the casing, towards the nose, resulting from the presence of the inert components of the auxiliary detonator. For Composition A, the coarsely fragmented region does not extend so far down the casing (compare Plates 7 and 8). If for TNT the nose half of the shell had a fragment mass distribution more like the observed distribution of the base half, the value of M_0

Figure 3

Mk. 27-3 3"A.A. Projectile, Lot 18+2, with Mk. 51 M.T. fuze and Mk. +6 auxiliary detonator
Cast TNT

○ Shot #18
△ Shot #21

Straight line corresponds to empirical equation:

$$N_1 = 399 \exp\left(-\frac{M_1}{2.19}\right)$$

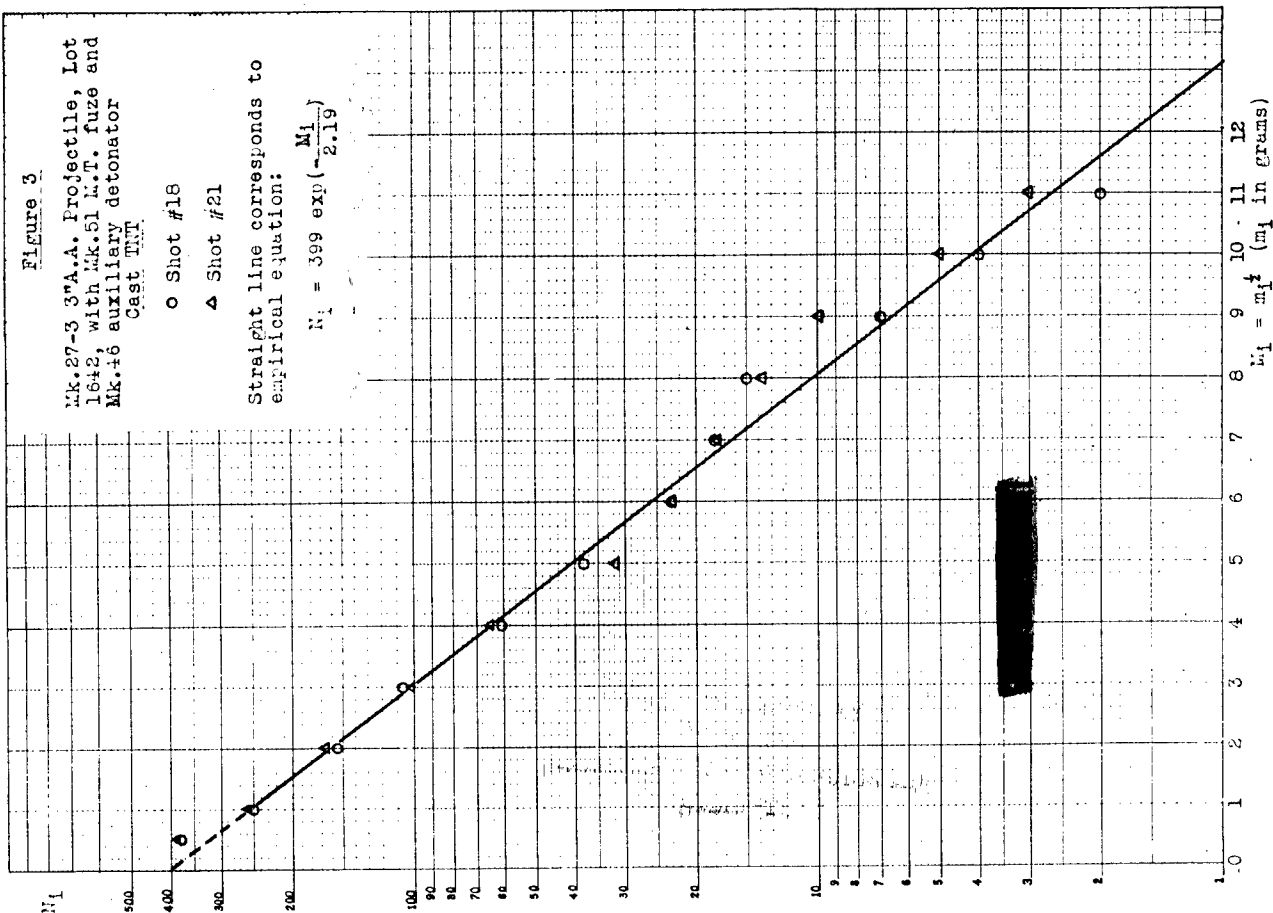


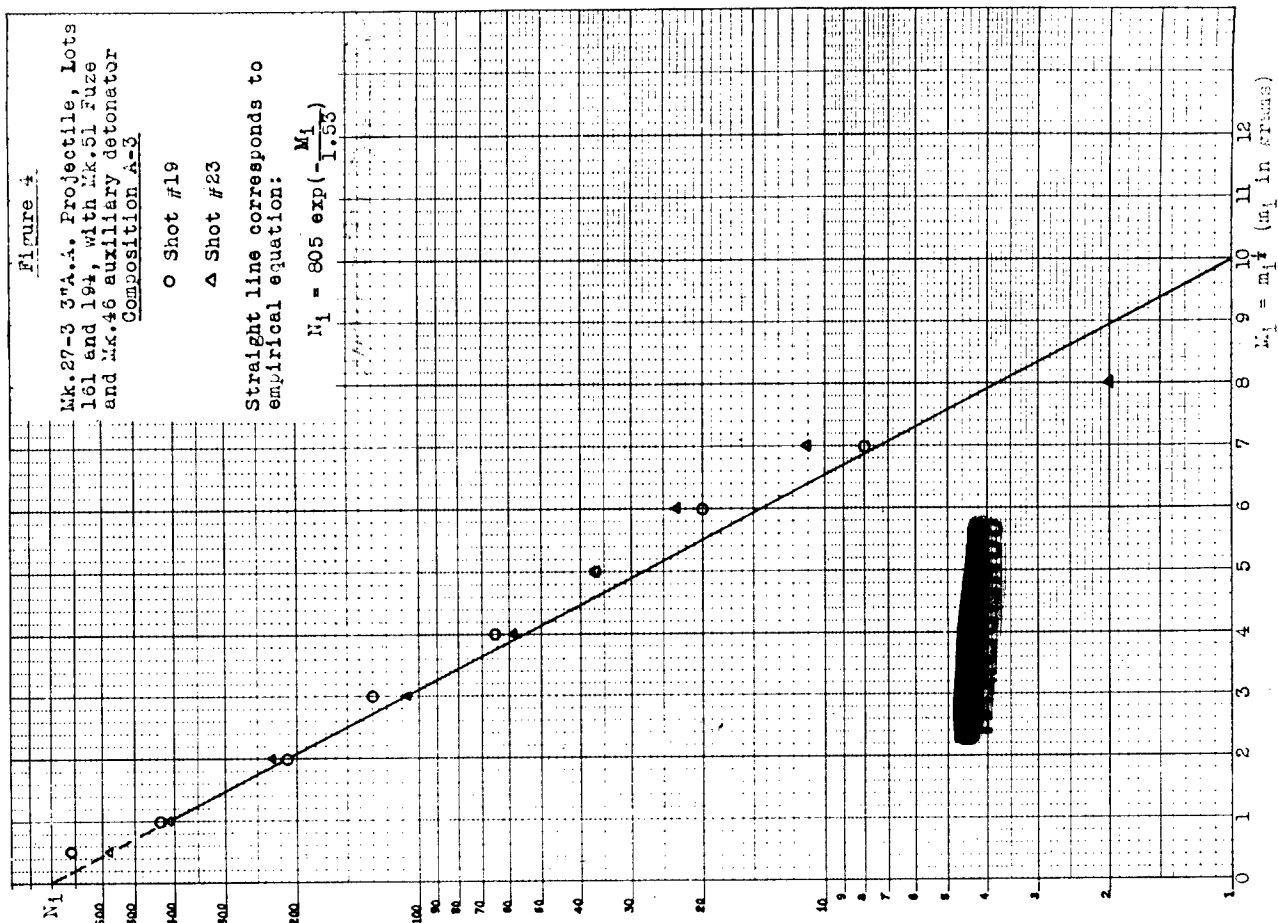
Figure 4

Mk. 27-3 3"A.A. Projectile, Lots 161 and 194, with Mk. 51 Fuze and Mk. +6 auxiliary detonator
Composition A-2

○ Shot #19
△ Shot #23

Straight line corresponds to empirical equation:

$$N_1 = 805 \exp\left(-\frac{M_1}{1.53}\right)$$



[REDACTED]

would be closer to the theoretically calculated one. The nose fragments do in fact have greatly reduced velocities compared with the lower side-wall fragments.

The mean thickness of central side-wall fragments showing both inner and outer surfaces was between 0.37" and 0.38" for the TNT-loaded shell and about 0.40" and 0.39" for the Composition A-loaded shell. Comparing these figures with the original casing thickness of 0.54", we may infer that this part of the casing expanded by about 44% before rupture in the case of TNT and 35-38% in the case of Composition A. The difference is small and may be not significant, particularly in view of the fact that the shell come from different lots.

[REDACTED]

Three shell from the same lot, also tested for hardness, were fragmented with loadings of Aluminized Composition A (73-18-9 RDX/Aluminum/Wax). The object was to determine whether there was any advantage of this composition over ordinary Composition A.

The shell were loaded in the following way. Four preformed pellets, of diameter just large enough to slide in the casing, were inserted in the shell and consolidated by pressure. The level of the explosive was then adjusted to the bottom of the auxiliary detonator cavity by adding a thin layer of explosive, where necessary, and pressing again. The detonator cavity was then preformed by inserting a brass slug of the proper size and pressing explosive around it by means of a hollow cylindrical plunger. The pressure was 10,000 psi. throughout. The shell were cavitized to receive the dummy Mk. 51 fuze and the Mk. 54 auxiliary detonator, as in the case of the TNT-loaded shell discussed in Section a). The charge density was 1.75 for 50-50 Potassium Nitrate/Composition A and 1.69 for 73-18-9 RDX/Aluminum/Wax.

The data are given in Table VI. The fragments for one shell of each type are shown in Plates 9-12. In Shot No. 61, the base came off in one single fragment instead of breaking up into smaller pieces. The fragmentation of this shell was otherwise not extraordinary.

Table VI

Mk. 27-3 3" A. A. Projectile, 50-50 KNO₃/Composition A
and Composition A/Al, Mk. 51 MT Fuze and Mk. 54 Aux. Det.

<u>Initial data:</u>	<u>KNO₃/Comp.A</u>		<u>Comp.A/Aluminum</u>		
	<u>No. 58</u>	<u>No. 59</u>	<u>No. 60</u>	<u>No. 61</u>	<u>No. 62</u>
Hardness, Rockwell C	26.4	26.3	26.3	26.3	26.0
Total weight, loaded shell without fuze or adapter	4515g.	4528g.	4526g.	4500g.	4505g.
Charge weight	4000	404	397	381	391
Casing weight	4115	4124	4129	4119	4114
Copper rotating band*	204	204	204	204	204
Casing steel	3911	3920	3925	3915	3910
Fuze adapter	357	356	358	357	356
Mk. 54 auxiliary detonator	994	999	990	998	999
+ Mk. 51 fuze					
Booster weight	15	15	15	15	15
Metal parts, fuze + aux. det. + adapter	1336	1340	1333	1340	1340
<u>General recovery data:</u>					
Casing steel fragments**	3938	3921	3922	3906	3858
Weight of all fragments > 1 gram	3834	3820	3740	3762	3706
Copper fragments from rotating band	185	202	198	191	191
Fragments from fuze, aux. det. and adapter	1321	1303	1310	1304	1324

*Nominal value

**May include a small quantity of fragments from fuze, auxiliary
detonator or adapter, not identifiable as such.

Table VI (continued)

KNO ₃ /Comp.A		Comp.A/Aluminum		
<u>No. 58</u>	<u>No. 59</u>	<u>No. 60</u>	<u>No. 61</u>	<u>No. 62</u>

Detailed recovery data:

Casing steel fragments

No. with mass > 196 grams		0		**1	
169		1		1	
144		1		1	
121		5	0	1	
100	0	5	1	1	0
81	3	7	1	3	1
64	9	13	5	5	5
49	18	15	11	9	10
36	27	21	17	17	24
25	46	35	27	32	40
16	69	57	62	53	69
9	121	113	134	108	125
4	184	177	224	216	183
1	284	288	387	385	346
0.25	365	359	557	557	480
Average mass of fragments > 1 gram	13.50	13.26	9.66	9.67	10.71
$\frac{M_o}{AM_o}$	2.05 463	2.03 471	1.64 712	1.66 703	1.76 611
$\sum X^2$	6.59	10.78	13.67	4.67	11.39

Copper rotating band fragments

No. with mass between 0.25 and 10 grams	34	55	89	96	87
---	----	----	----	----	----

Fuze, aux. det. and adapter fragments

No. with mass > 100 grams	4	3	3	5	4
between 49 and 100	2	2	2	1	2
between 9 and 49	9	11	8	8	12
between 0.1 and 9	75	74	106	86	99

*See Appendix I

**Base plug, 302 g., in one piece.

The data for 50-50 KNO_3 /Composition A are in fairly good agreement for the two shell, though No. 59 gave a few larger fragments. The results are plotted graphically in Figure 5, together with the line corresponding to the empirical equation:

$$N_i = 467 \exp \left(- \frac{M_i}{2.04} \right)$$

One sees that the distributions are practically identical with those for cast TNT (Table II).

For aluminized Composition A, the data are not so consistent. Shell Nos. 60 and 61 are in good agreement with each other, but the distribution for No. 62 is somewhat coarser. Nos. 61 and 62 are consistent with the exponential law, but the hypothesis is rejected for No. 60 at 5% significance level, though not at 1%. The results are plotted in Figure 6, together with the average line corresponding to the empirical equation:

$$N_i = 675 \exp \left(- \frac{M_i}{1.69} \right)$$

Comparing with Table V, bearing in mind, however, that the shell in that table were from different lots, one sees that the fragmentation is coarser for the aluminized Composition A than for the aluminized Composition A than for straight Composition A, though still appreciably finer than for TNT (see Table II for exact comparison). According to the theory of shell fracture. The coarse fragmentat pattern should correspond to a lower casing expansion velocity. We noted, however, that several of the fragments from these shell passed entirely through the sawdust and marked the walls of the fragmentation pit. This did not happen with any other type of 3" shell fired, including the ones loaded with straight Composition A. Therefore the aluminized Composition A apparently gives rise to some unusually energetic fragments. It will be interesting to determine the fragment velocities with this filling. If these should turn out to be greater than for straight Composition A (just as those for Torpex are greater than those for Composition B), the anomaly could be explained on the basis of the supposition that for the aluminized composition there continues to be acceleration of the fragments by the explosion products after break-up, i.e., part of the total energy is released after the casing has expanded to the point of rupture. In a sufficiently large charge, this presumably would not occur and there should then be a closer correlation between velocity and mean fragment size.

Figure 5

Mk.27-3 3" A.A. Projectile, Lot 1350, Mk.51 fuze with Mk.54 auxiliary detonator

50-50 KNO₃/Composition A

○ Shot No.58
△ Shot No.59

Straight line corresponds to empirical equation:

$$N_1 = 467 \exp\left(-\frac{M_1}{2.04}\right)$$

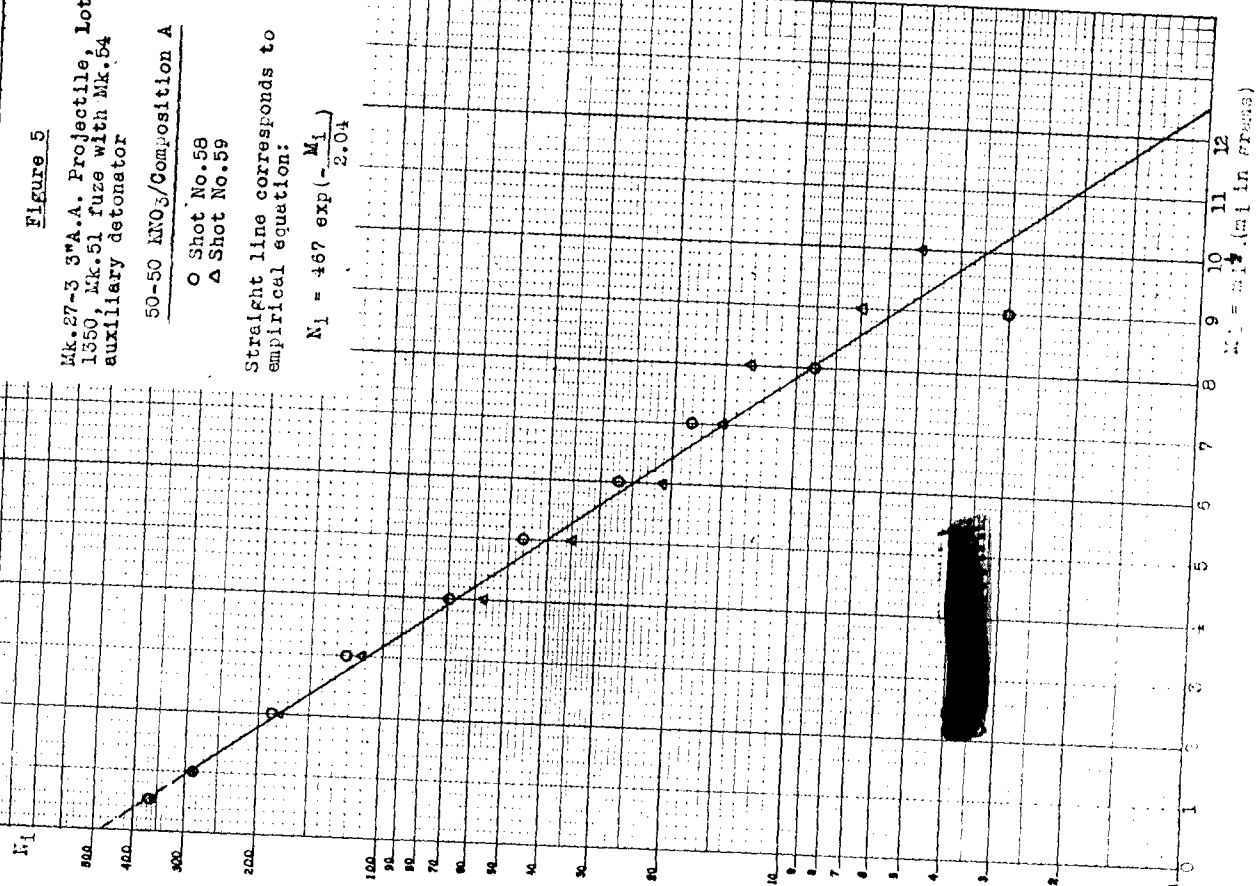


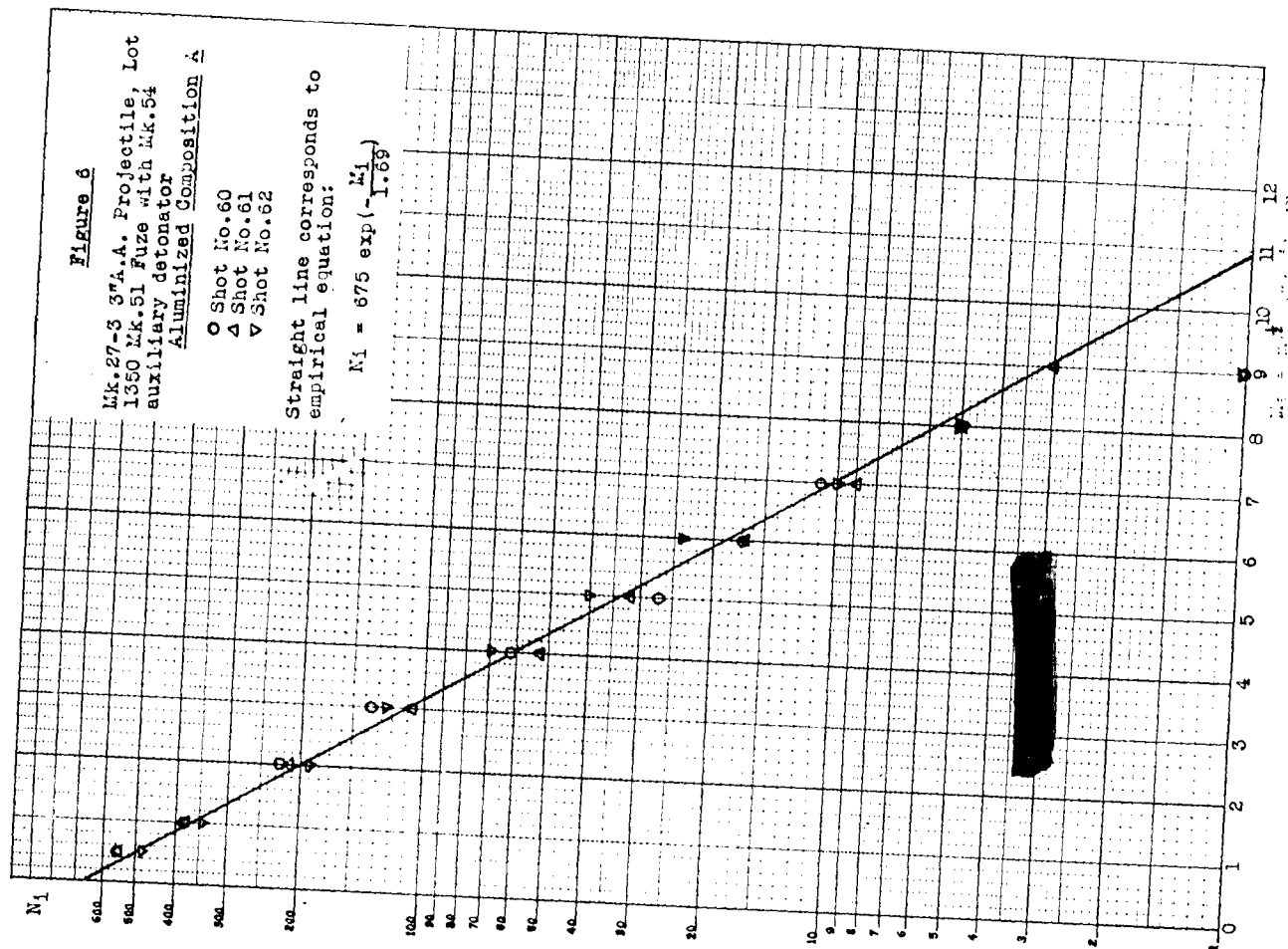
Figure 6

Mk.27-3 3" A.A. Projectile, Lot 1350 Mk.51 Fuze with Mk.54 auxiliary detonator
Aluminized Composition A

○ Shot No.60
△ Shot No.61
▽ Shot No.62

Straight line corresponds to empirical equation:

$$N_1 = 675 \exp\left(-\frac{M_1}{1.69}\right)$$



[REDACTED]



The shell were all taken from Lot No. 1350, but since this investigation was started before hardness and other mechanical properties had been determined, no individual hardness measurements were taken. For this reason, the interpretation is open to some question.

Since we wanted to be sure that the main charges were adequately boosted, we used pressed 25 gram Teteryl pellets in place of the 15 gram boosters used in the service Mk. 46 and Mk. 54 auxiliary detonators. The shell were loaded with the aid of 8" long aluminum riser tubes to the shoulders seating the threaded fuze adapter rings and drilled to a depth of about 2 mm. to receive the uncased 1-1/4" diameter pellets, which were set within the lower threaded sections of the adapters that normally receive the auxiliary detonators. The shell were closed with brass end-plugs weighing about 670 grams, drilled axially to receive No. 8 duPont electric detonators and screwed into the upper threaded sections of the adapters in place of fuzes. One of the TNT-loaded shell, No. 32, was fired with only a light wooden plug to hold the detonator, in place of the heavy brass end-plug. This was done to test whether the method of closure affected the fragmentation pattern. The fragment mass distribution for this shell was practically indistinguishable from those of other TNT-loaded shell, except that the adapter ring was not fractured.

the sawdust was run through the separator again at three-fourths the normal speed. A total of 111 grams of steel was recovered, of which 98 grams consisted of material passing through a U. S. No. 20 standard sieve, i.e., the individual particle mass was probably not greater than 0.005 grams. The new separator (Dings Type F-A with magnetized drum; see Plate 2) is much more efficient, but we believe that even with the old machine, recovery was complete down to 0.25 gram individual mass.

Table VII

Mk. 27-3 3" Projectile, TNT, TNT-D2 and Picratol, Brass End-plug and Uncased 25-Gram Teteryl Booster in place of Conventional Fuze and Auxiliary Detonator

	TNT				TNT-D2				Picratol			
	#30	#31	#32	#42	#33	#34	#40		#35	#38	#41	
Initial data:												
Total weight, loaded shell, without end-plug or adapter	4584	4576	4574	4575	4576	4572	4562	(All weights expressed in grams)	4591	4588	4581	
Charge weight, main charge	435	435	432	437	421	425	422		441	437	436	
Booster	25	25	25	25	25	25	25		25	25	25	
Casing weight	4124	4116	4117	4113	4130	4122	4115		4125	4126	4120	
Rotating band (copper)*	204	204	204	204	204	204	204		204	204	204	
Casing steel	3920	3912	3913	3909	3926	3918	3911		3921	3922	3916	
Adapter steel	358	356	357	358	356	358	356		356	356	358	
End-Plug (brass)	674	671	None	666	656	661	664		681	670	670	
General recovery data:												
Casing steel fragments**	3916	3948	3894	3926	3968	3942	3863		3895	3901	3990	
Weight of all fragments > 1 gram	3746	3717	3773	3752	3784	3794	3724		3765	3795	3804	
Copper fragments from rotating band	201	203	201	206	193	202	204		197	189	194	
Adapter fragments	336	274	362	342	361	343	342		373	283	334	
End-plug	668	668	--	662	652	660	661		676	661	666	

* Nominal value

** May in some cases include a few very small particles from adapter, not identifiable as such.

Table VII (Continued)

	TNT			TNT-D2			Picratol		
	#30	#31	#32	#42	#33	#34	#35	#38	#41
Detailed recovery data:									
Casing steel fragments									
No. with mass > 144 grams									
121		0	2		1	0	0	0	0
100	0	3	4		2	1	1	1	1
81	2	4	4	0	3	1	2	2	2
64	2	10	5		5	6	3	4	5
49	14	17	11	1	8	13	9	10	7
36	24	28	16	11	15	16	17	17	19
25	43	39	23	25	26	20	28	28	33
16	74	62	35	47	40	42	43	45	39
9	134	107	57	64	64	69	64	62	63
4	193	180	109	119	117	115	108	107	113
1	293	306	169	212	179	175	176	174	179
0.25	481	539	296	372	287	298	307	301	300
			407	551	485	468	449	440	486
Average mass of fragments									
with individual mass > one gram									
1	12.78	12.15	12.75	10.09	13.18	12.73	12.26	12.61	12.68
Mo	1.98	1.91	1.98	1.69	2.02	1.97	1.92	1.96	1.97
AM ₂ *	485	516	491	672	471	495	516	501	498
\bar{x}	24.44	3.18	6.89	20.89	5.20	12.23	3.04	5.32	15.79
	(13.72)			(11.26)					(10.93)

*For significance see Appendix I. Values in parentheses are for five degrees of freedom, grouping all fragments above 49 grams in one class. All other values are for six degrees of freedom, including a class between 49 and 64 grams as well as a class of all fragments greater than 64 grams.

Copper rotating band
fragments 9-16 grams
0.25 - 9

2 0 1 3 0 0 0 0 0 0
70 67 79 79 59 56 75 79 82 79

Table VII (Concluded)

Table VII (Continued)								
TNT		TNT-D2		Picratol				
#30	#31	#32	#12	#33	#34	#40	#35	#38
								#41
5	3	0	5	7	6	5	7	5
10	13	1	8	8	10	8	9	11
11	5	0	10	11	15	13	14	8
(41 piece)(41 piece)								
(349 g.) (57 g.)								

Adapter fragments

These data are fairly consistent with the exception of Shot #42 for TNT. This shot gave many more fragments and a generally finer mass distribution than the other TNT-loaded shell. It is unfortunate that we did not have mechanical property tests of the shell at the time this series was fired. The data would be brought into line if it could be shown, for example, that Shell #42 had an exceptionally great hardness and associated brittleness. In the absence of such information, we have little choice but to eliminate Shell #42 from the comparison on the arbitrary basis that the results are not consistent with those of the other three shell.

The other three TNT-loaded shell gave rather widely varying numbers of fragments down to 0.25 gram. Down to 1 gram, however, the data are in fairly good agreement, with Shot #30 showing a somewhat finer distribution than the others. The distribution for Shot #30, according to the Chi-square test, is inconsistent with the exponential law at significance level of 1%. The departure is most prominent in the range of large fragments, the actual numbers of which are too small in relation to the numbers of smaller fragments to be consistent with the law. This is shown by the fact that when all fragments with masses equal to or greater than 49 grams are grouped in a single class, without reference to the detailed distribution within that class, the observed distribution appears to be in much better agreement with the law. A similar remark applies with even greater force to Shot #41 (Picratol) where when the number with masses between 49 and 64 grams and the number with masses equal to or greater than 64 grams are treated as separate classes (the method generally followed in this report; see Appendix I), the exponential law is rejected at significance level of 5% (though not at 1%), but when all fragments with masses equal to or greater than 49 grams are grouped in a single class, the hypothesis becomes not inconsistent with the observed distribution at this level of significance. Evidently the distribution of the larger fragments is in this case the major source of deviation from the exponential law.

If Shot #42 is removed from consideration, the three explosives show indistinguishable fragment mass distributions. Table VIII presents average cumulative numbers of fragments and also the average values of \bar{L}_0 , together with their average deviations. One sees that nowhere are the differences among the averages for the three explosives significant in comparison with the deviations among the results for a given explosive.

Table VIII

Averages for TNT, TNT-D2 and Picratol, Mk. 27-3 3" Projectile

No. steel casing fragments with masses equal to or greater than:		TNT	TNT-D2	Picratol
		##30, 31, 32	33, 34, 40	##35, 38, 41
100 grams		2 ± 2	2 ± 1	2 ± 0
81		4 ± 1	4 ± 2	4 ± 1
64		8 ± 4	9 ± 2	9 ± 1
49		16 ± 1	16 ± 0	18 ± 1
36		25 ± 2	25 ± 4	30 ± 2
25		39 ± 3	41 ± 1	42 ± 2
16		64 ± 6	65 ± 3	63 ± 1
9		117 ± 12	114 ± 3	109 ± 2
4		181 ± 8	177 ± 2	176 ± 2
1		298 ± 5	296 ± 6	303 ± 3
0.25		476 ± 46	476 ± 6	458 ± 18
M ₀ :		196 ± 0.03	1.96 ± 0.04	1.95 ± 0.02

In Figure 7, we have plotted the average data in Table VIII for each type of loading (with exclusion of Shot #42) and also the line corresponding to the exponential equation:

$$N_i = 498 \exp \left(- \frac{M_i}{1.96} \right)$$

According to the fragment velocity measurements previously referred to, the average fragment velocities for TNT and Picratol were indistinguishable, but the average for TNT-D2 was about 6% lower. The steel panel penetrations for TNT-D2 were also slightly poorer than for the other two explosives. Mott has given theoretical reasons for supposing that the value of M₀ for a given shell should vary in inverse proportion to some power close to the two-thirds of the initial fragment velocity (see Equation 5). The observed difference of 6% between TNT and TNT-D2 would lead us to expect a possibly coarser distribution for TNT-D2 corresponding to M₀ greater by about 4%. Such a difference would probably be too small to be detected even with a large number of shots, for we have seen that the ten uniform TNT-loaded shell (discussed in Section a), gave a standard deviation in M₀ of about 4.4%. Unless the difference between the averages for two such sets of observations were at least twice this, or about 9%, we should be unable to distinguish them at confidence level of 95%.

Figures for Picratol in comparison with TNT are given in Picatinny Arsenal Report No. 1530 by G. M. Hopkins. In the 90 mm. shell, M71, Picratol gave 769 ± 32 fragments as compared with

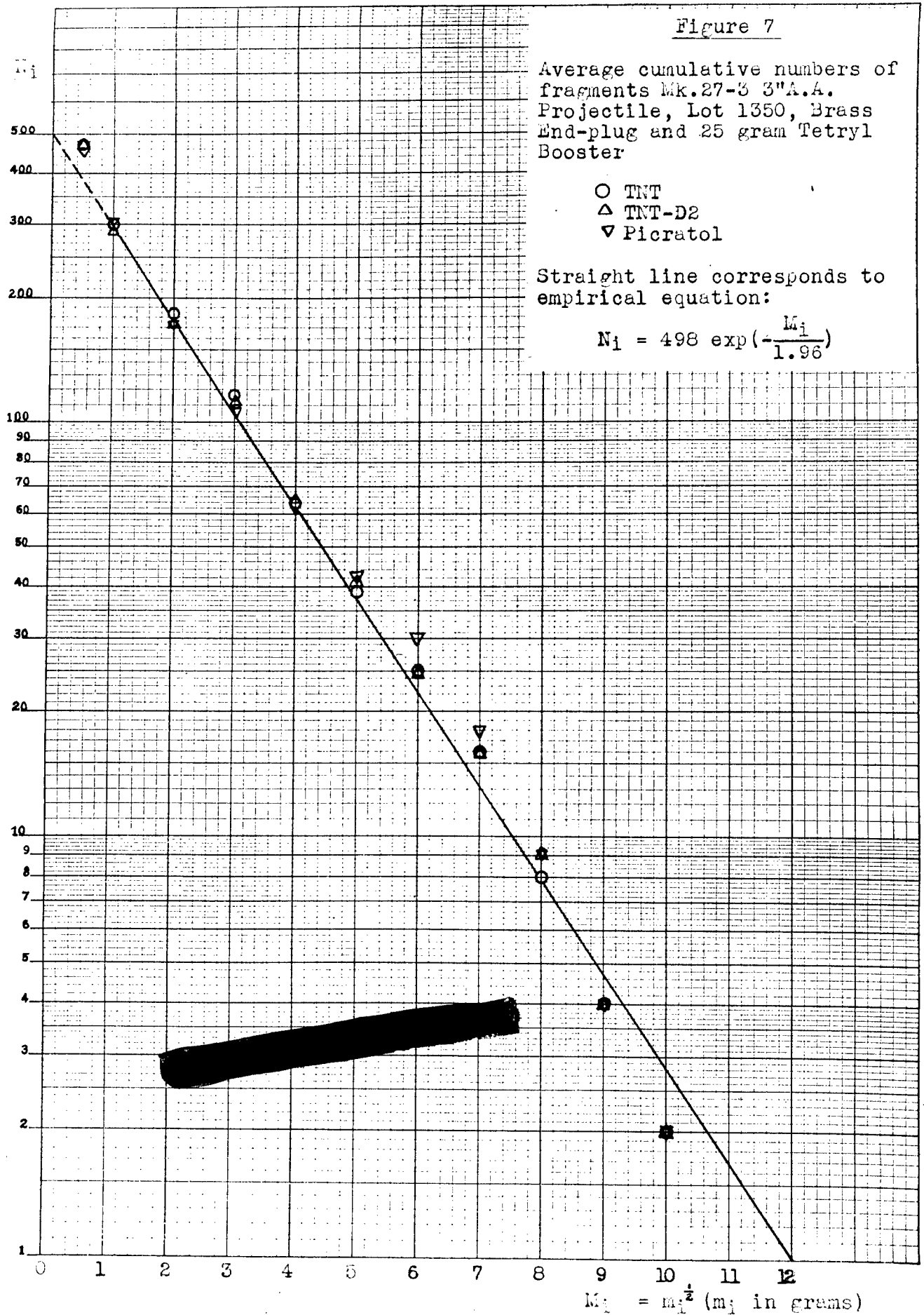
Figure 7

Average cumulative numbers of fragments Mk.27-3 3"A.A.
Projectile, Lot 1350, Brass
End-plug and 25 gram Teteryl
Booster

- TNT
- △ TNT-D2
- ▽ Picratol

Straight line corresponds to
empirical equation:

$$N_i = 498 \exp\left(-\frac{M_i}{1.96}\right)$$



[REDACTED]

703 \pm 24 for TNT. In the 3" shell, M42A1, on the other hand, Picratol gave 487 \pm 23 as compared with 514 \pm 18 for TNT. (These totals are numbers retained on a 4-mesh screen, which includes 98-99% of the original casing mass; the smallest fragment retained would be the order of 0.8 gram in individual mass.) The conclusion reached was that the two explosives were in the same group with respect to order of effectiveness.

A rather unexpected finding in the present investigation was that both the values of M_0 and the observed actual numbers of fragments for TNT (e.g., down to 1 gram individual mass) were almost the same from these shell as from the shell described in Table II that were cavitized to take the Mk. 54 auxiliary detonator, despite the fact that the detonator cavity is responsible for reducing the main charge by about 15%.

2. Mk. 31-1 3"/50 A.A. Projectile

At the request of the Bureau of Ordnance, we have fragmented ten Mk. 31-1 3" A.A. projectiles loaded with cast TNT and ten loaded with pressed Composition A-3, half of them cavitized to receive the Mk. 58 VT fuze and Mk. 44 auxiliary detonator and half to receive the longer Mk. 45 VT fuze and Mk. 44 auxiliary detonator. All of the shells were from a common lot, Lot No. 138-37, but they were received service-loaded (from NAD, Fort Mifflin), and individual hardness tests were therefore not made. The object was to compare the two explosives under the service loading conditions in this shell, normally equipped with one of the VT fuzes occupying a relatively large part of the casing.

The Mk. 31-1 projectile differs from the Mk. 27-3 in certain minor respects. It has no tracer cavity in the base and instead of having a removable fuze adapter, the nose itself is threaded directly to receive the VT fuzes, which are larger in diameter than the MT fuzes. The o.d. over the main body is 2.95", the bourrelet at the shoulder being slightly larger, 2.985". The o.d. of the Mk. 27-3 projectile is 2.98" with no bourrelet. In both projectiles, the explosive cavity is cylindrical with diameter 1.90" over practically its entire length, so that the casing wall thickness is slightly smaller for the Mk. 31-1, 0.525" as compared with 0.540". There has been in existence also a so-called EX-2 3" A.A. projectile, consisting of the Mk. 27-3 with the nose rethreaded to receive a larger adapter that takes the VT fuzes. A parallel investigation of fragment velocities and panel penetrations for the same two explosives and same two fuzes has been carried out at this laboratory by R.W. Drake using the EX-2 projectile (OSRD Reports Nos. 5266 and 5267).

There is a difference in the way in which the Mk. 31-1 projectile is loaded as compared with the Mk. 27-3. Due to the large diameters of the VT fuzes, there is just room for them within the casings, with no explosive at all surrounding them. For the Mk. 58 fuze, the first 3-1/2" from the nose and for the Mk. 45 fuze, the first 4-1/4" of the 8-1/2" casing length therefore contain no explosive at all. The main charge, beginning at these respective levels, is further cavitized over 3/4" length to receive the booster cup of the Mk. 44 auxiliary detonator. The main charge with the Mk. 58 fuze is thus 24% less and with the Mk. 45 fuze 38% less than in the case of the Mk. 27-3 projectile with Mk. 51 MT fuze.

For these static shots, the fuzes contained no electronic parts but were initiated in the armed condition by an external electric firing circuit that fired the electric detonator normally present in the fuze. The auxiliary detonators were likewise armed for static initiation.

a) Composition A and TNT with Mk. 58 VT Fuze

The data for the Mk. 58 fuze are summarized in Table IX. The fragments recovered from representative shell with each type of loading are shown in Plates 16-19.

The recoveries were generally satisfactory except for the fuze parts. The fuzes and auxiliary detonators together contained between 90 and 100 grams of explosive and plastic parts but in some cases the recoveries were as much as 80 grams short even after allowing for the non-recoverable portions. A considerable fraction of this probably consisted of non-magnetic metal, of which a little more than 100 grams was present, that may have passed through the separator undetected. Much of this non-ferrous material is located just above the booster and is probably rather finely disintegrated.

One should note that Table IX (and also Table XI below) are constructed somewhat differently from Table II. Table IX gives directly the numbers of fragments within the various mass groups instead of the cumulative numbers. This has been done deliberately to bring out the obvious distinction between a relatively small number of massive nose fragments showing adapter threads, split from the region of the shell, containing no explosive, surrounding the inert fuze body, and the main bulk of fragments that have been subjected to direct explosive action. These nose fragments are readily distinguished in appearance from the others (see Plates 18 and 19) and are known in fact to have much lower velocities (OSRD Report No. 5266). When they are included in the total count, the fragment mass distribution as a whole departs widely from the exponential law. We have attempted to fit the exponential law to the high-velocity fragments by excluding the massive nose fragments (about 30% of the total casing mass) from the count. The fragments excluded were generally, though not without a few exceptions, the heaviest ones in the distribution. Table IX gives the average mass of all steel casing fragments with individual masses equal to or exceeding 1 gram, excluding the nose fragments. From this average mass, a value of M_0 has been calculated according to Equation (11). Table X gives the average cumulative numbers of fragments and their average deviations for each explosive, excluding the nose fragments, together with the numbers calculated according to the empirical exponential formulæ:

$$N_i = 424 \exp \left(- \frac{M_i}{1.82} \right) \quad (\text{TNT})$$

$$N_i = 841 \exp \left(- \frac{M_i}{1.31} \right) \quad (\text{Composition A})$$

[REDACTED]

where 1.82 ± 0.07 is the mean value of M_0 for the five TNT-loaded shell and 1.31 ± 0.04 is the mean value for Composition A. The agreement among the shell for either explosive is quite good, though #53 for TNT gave somewhat fewer fragments than the other similar shell. The average data from Table X have been plotted in Figures 8 and 9 (small circles) together with the lines corresponding to the empirical formulae given above. The large circles in Figures 8 and 9 represent the total cumulative numbers, including the massive nose fragments.

Figure 8

Average cumulative numbers of fragments Mk.31-1 3"A.A. projectile, Lot 138-37, TNT, Mk.58 VT Fuze

- All fragments
- Excluding average of 8 massive nose fragments

Straight line corresponds to empirical equation:

$$N_1 = 424 \exp(-\frac{M_1}{1.82})$$

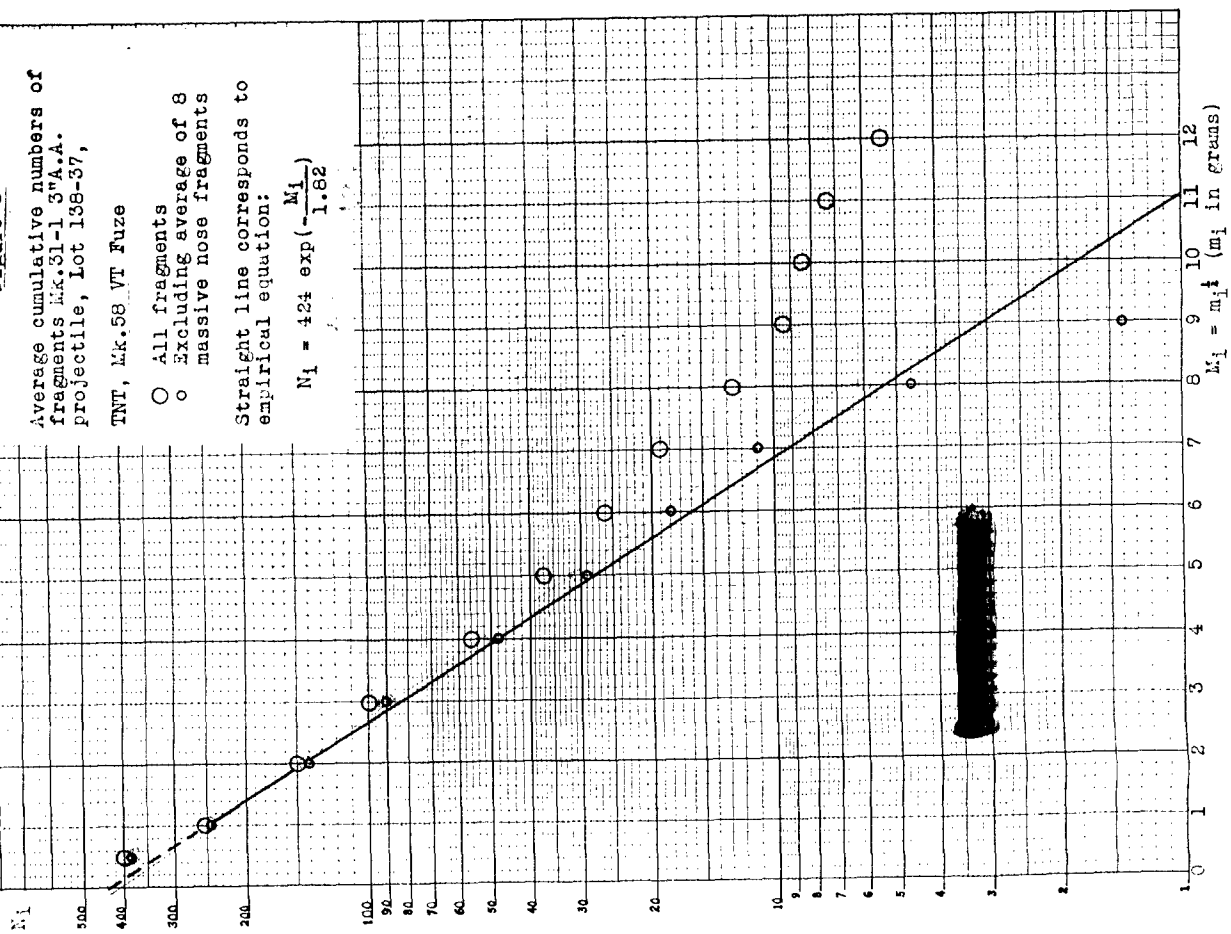


Figure 9

Average cumulative numbers of fragments Mk.31-1 3"A.A. Projectile, Lot 138-37, Composition A-3, Mk.58 VT Fuze

- All fragments
- Excluding average of 10 massive nose fragments

Straight line corresponds to empirical equation:

$$N_1 = 841 \exp(-\frac{M_1}{1.31})$$

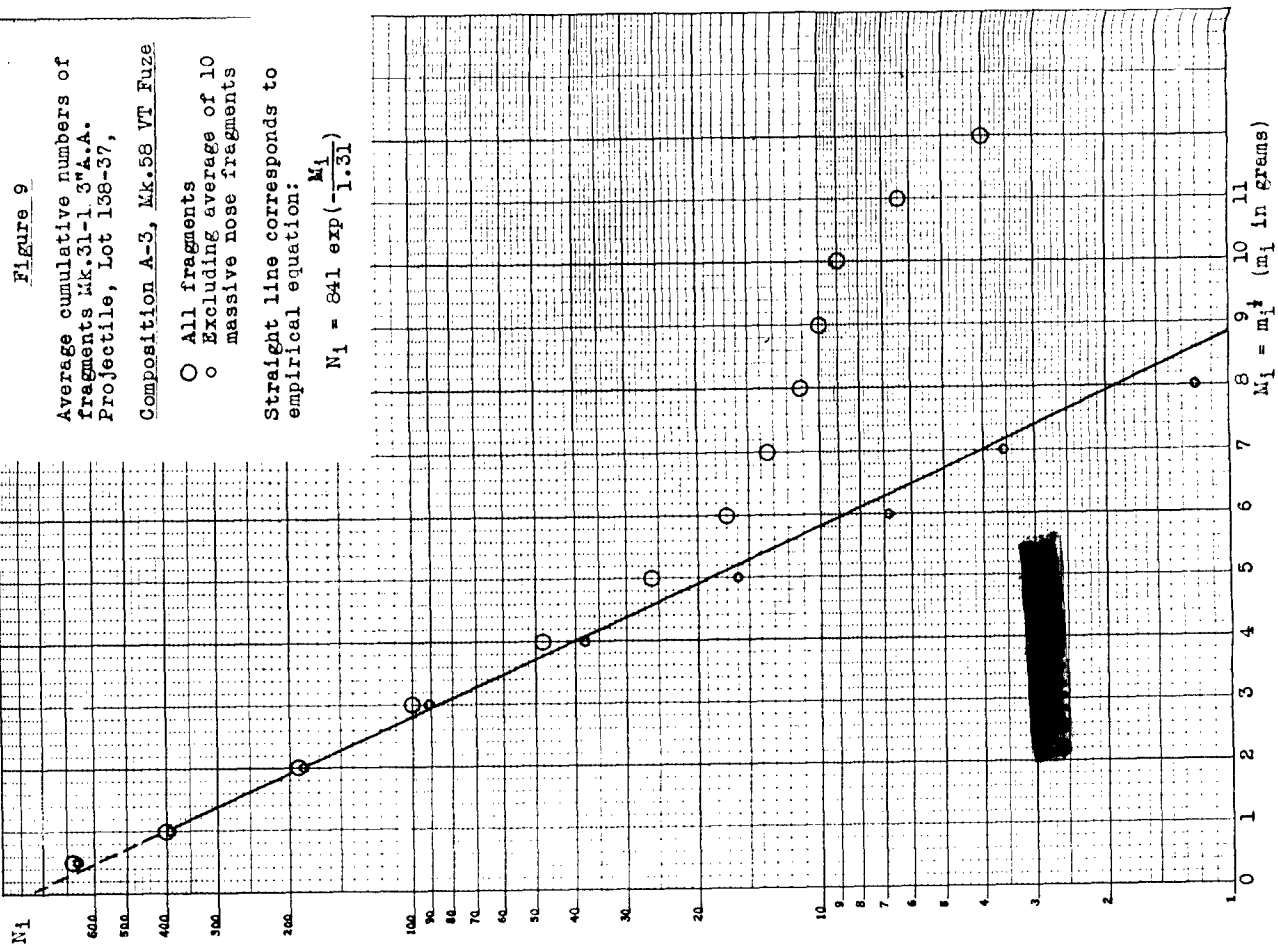


Table IX

Mk. 31-1 3" A.A. Projectile, TNT and Composition A-3, Mk. 58 VT Fuze, with Mk. 44 Auxiliary Detonator

Initial data:	TNT			Composition A-3						
	#46	#47	#52	#53	#54	#48	#49	#50	#51	#55
(All weights in grams)										
Total weight, loaded shell	4770	4766	4781	4765	4750	4779	4767	4789	4778	4800
without fuze										
Charge weight*	277	277	272	277	277	286	286	286	281	281
Casing weight	4493	4489	4509	4488	4473	4493	4481	4503	4497	4519
Copper rotating band**	204	204	204	204	204	204	204	204	204	204
Casing steel	4289	4285	4305	4284	4269	4289	4277	4299	4293	4311
Mk. 44 auxiliary detonator	210	214	215	213	215	211	210	213	214	213
Booster weight	25	25	25	25	25	25	25	25	25	25
Mk. 58 fuze	680	681	679	678	685	681	691	679	681	689
Metal parts, fuze / aux. det.	800	805	803	801	809	802	811	803	804	812
General recovery data:										
Casing steel fragments***	4332	4286	4288	4295	4269	4319	4254	4286	4315	4332
Weight of fragments > 1 gram	4188	4130	4122	4174	4125	4066	4049	4055	4050	4060
Copper fragments from rotating band	200	199	201	197	201	195	190	198	202	195
Fuze and aux. det. fragments	745	725	767	767	754	724	756	721	722	723

*Charge weights and empty casing weights as given by NAD, Fort Mifflin.

**Nominal value; casing steel weights may be in error by several grams due to variations in this quantity.

***May include a few small fragments from fuze or auxiliary detonator, not identifiable as such.

Table IX (continued)

		TNT						Composition A-3				
		#16	#17	#52	#53	#54	#18	#19	#50	#51	#55	
<u>Detailed recovery data:</u>												
<u>Casing steel fragments</u>												
No. with mass:	225-256g.	2	2	0	0	2	0	0	0	0	1	
	196-225	3	0	3	1	0	0	0	0	0	1	
	169-196	1	1	0	4	1	1	2	0	1	2	
	144-169	0	1	0	2	4	2	2	3	2	2	
	121-144	1	3	3	2	0	3	3	4	3	0	
	100-121	1	1	1	0	1	1	2	3	4	2	
	81-100	0	2	2	0	2	2	1	0	1	0	
	64-81	5	5	2	5	0	3	3	0	0	1	
	49-64	5	7	6	4	8	4	5	1	3	0	
	36-49	4	6	12	6	9	3	5	0	2	6	
	25-36	17	11	7	11	10	13	4	12	7	12	
	16-25	15	19	26	17	16	16	18	26	24	23	
	9-16	43	33	51	46	40	56	44	64	52	49	
	4-9	51	49	42	53	55	82	92	100	87	100	
	1-4	115	103	123	73	107	201	199	213	254	178	
	0.25-1	137	138	144	117	162	292	241	255	280	294	
No. course nose fragments		8	7	8	9		10	10	10	11	9	
Mass of nose fragments		1512g.	1241g.	1195g.	1584g.	1400g.	1242g.	1382g.	1329g.	1437g.	1427g.	
Average mass of fragments > 1 gram, excluding nose fragments		10.49	12.24	10.84	12.05	11.03	7.49	7.21	6.55	6.09	7.21	
M ₀ excluding nose fragments		1.74	1.92	1.77	1.90	1.79	1.37	1.33	1.24	1.27	1.33	
<u>Copper rotating band fragments</u>												
No. with mass 0.1 - 16g.		63	67	71	70	65	94	106	101	100	75	
<u>Fuze and aux. det. fragments</u>												
No. with mass > 350g.		1	1	1	1	1	1	1	1	1	1	
No. with mass 49-100g.		0	1	0	1	1	0	0	0	0	0	
No. with mass 9-49 g.		9	7	6	8	6	6	6	6	4	5	
No. with mass 0.1-9 g.		119	99	171	124	155	122	203	165	180	180	

Table X

Average cumulative numbers of steel casing fragments excluding massive nose fragments - Mk. 31-1 3" A.A. projectile, Mk. 58 fuze with Mk. 44 auxiliary detonator.

mi (grams)	TNT			Composition A-3		
	N_i (av. obs.)	N_i (calc., empirical exponential law)	Difference N_i (obs.) - N_i (calc.)	N_i (av. obs.)	N_i (calc., empirical exponential law)	Difference N_i (obs.) - N_i (calc.)
100	0.4	1.7	-1.3			
81	1.4±0.9	3.0	-1.6	0		
64	4.6±1.7	5.1	-0.5	1.2	1.9	-0.7
49	11±2	9	+2	3.6±2.7	4.0	-0.4
36	18±3	16	+2	6.8±3.4	8.6	-1.8
28	29±2	27	+2	16±3	18	-2
16	48±4	47	+1	38±2	40	-2
9	90±6	81	+9	91±6	85	+6
4	140±3	141	-1	183±11	182	+1
1	245±15	(245)	(0)	392±24	(392)	(0)
0.25	384±25	322	+62	664±22	574	+90

b) Composition A and TNT With Mk. 45 VT Fuze

The data for the Mk. 45 fuze are summarized in Table XI. The fragments recovered from representative shell with each type of loading are shown in Plates 20 - 23.

Shell #64 (TNT) gave a fragment mass distribution much coarser than those of the other TNT-loaded shell. This is the kind of behavior we might expect if the physical properties of this particular casing were below normal. We have excluded #64 from the average. The other shell gave generally consistent results.

As in the case of the Mk. 58 fuze, a small number of massive nose fragments were produced from the part of the shell containing no explosive. As expected, the combined mass and average mass of these fragments was greater than in the case of the Mk. 58 fuze, reflecting the greater length of the Mk. 45 fuze. We have attempted to fit exponential laws to the high-velocity fragments remaining after the massive nose fragments (about 37% of the total casing mass) were excluded. When the nose fragments were excluded, the next most massive fragment in the case of TNT was generally from the base, which in three of the five shots came off in one piece. The base fragments were, however, retained in the count in order to keep the treatment for TNT and for Composition A alike. Table XII gives the average cumulative numbers of fragments and their average deviations for each explosive, excluding the nose fragments, together with numbers calculated according to the empirical exponential formulae:

$$N_i = 405 \exp \left(- \frac{M_i}{1.78} \right) \quad (\text{TNT})$$

$$N_i = 690 \exp \left(- \frac{M_i}{1.36} \right) \quad (\text{Composition A})$$

where 1.78 ± 0.04 and 1.36 ± 0.05 are the respective values of M_0 for TNT and for Composition A. The data from Table XII

(small circles) together with the lines corresponding to the empirical exponential equations are shown graphically in Figures 10 and 11. The large circles represent the total cumulative numbers, including the nose fragments.

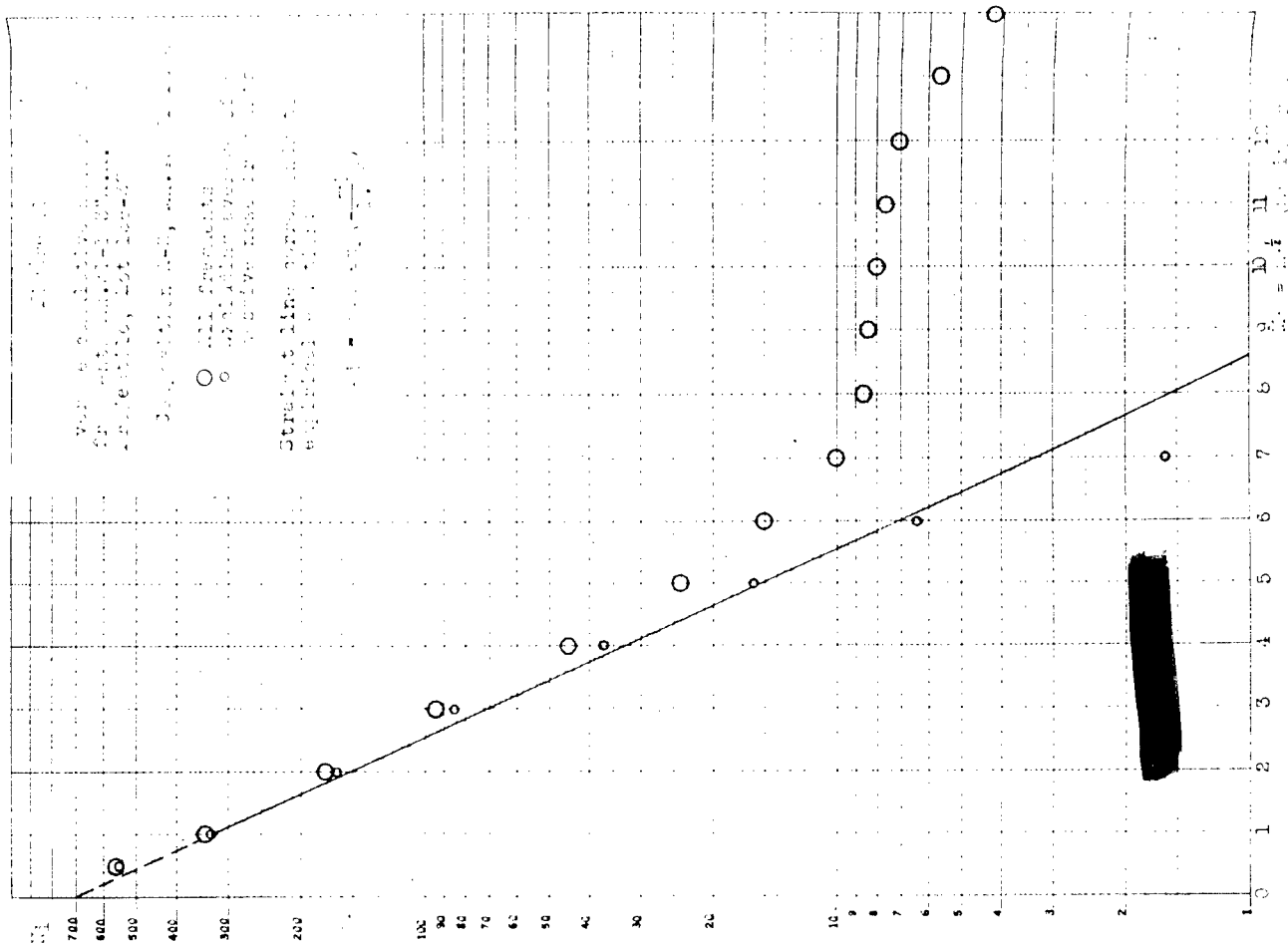
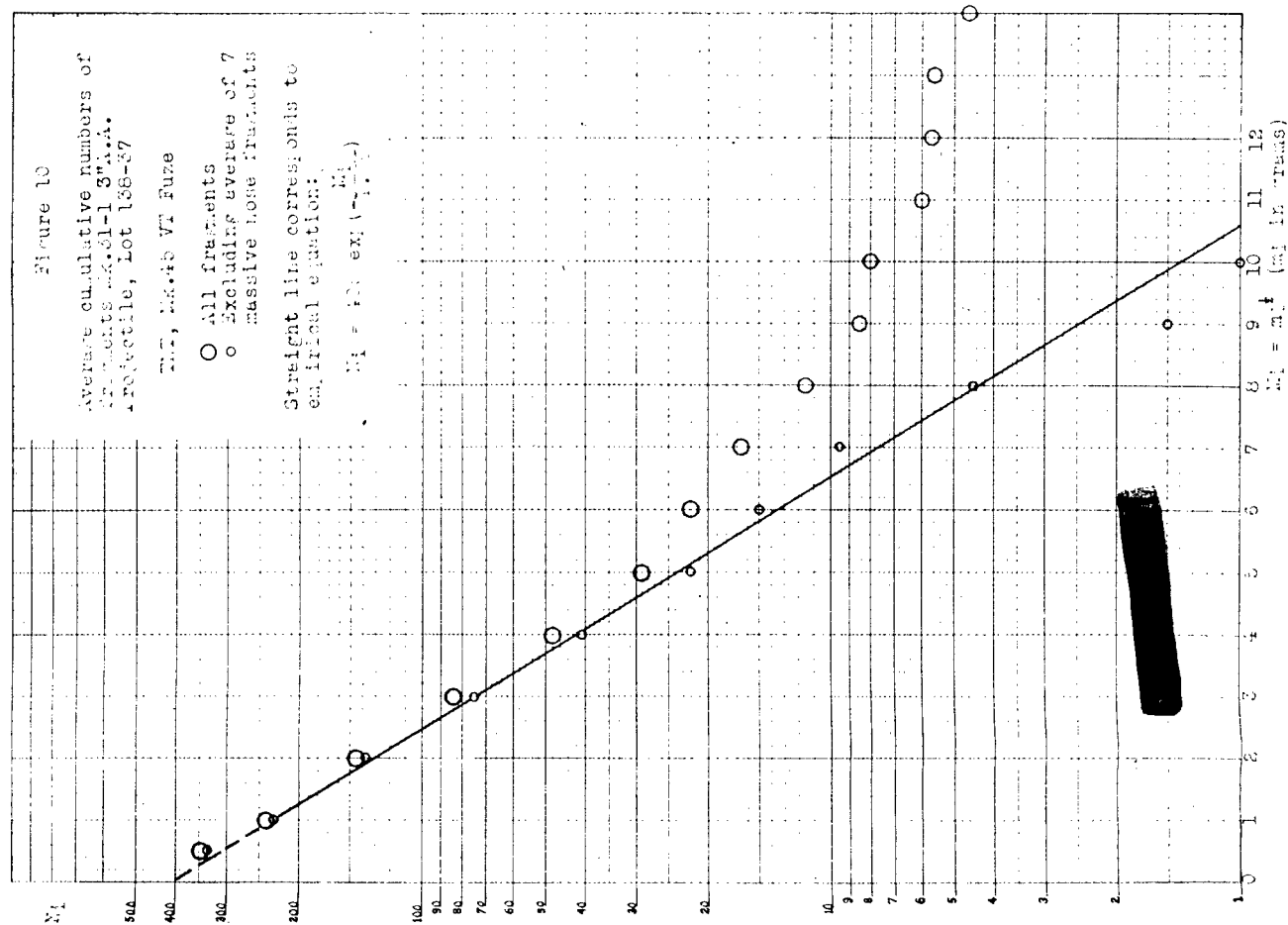


Table XI

Mk. 31-1 3" A.A. Projectile, TNT and Composition A-3, Mk. 45 VT Fuze with Mk. 44 Auxiliary Detonator

Initial data:	TNT				Composition A-3					
	#56	#63	#64	#65	#69	#57	#66	#67	#68	#72
(All weights in grams)										
Total weight, loaded shell without fuze	4702	4714	4719	4707	4722	4731	4724	4734	4753	4726
Charge weight*	222	222	227	227	227	231	227	236	240	231
Casing weight	4480	4492	4492	4480	4495	4500	4497	4498	4513	4495
Copper rotating band**	204	204	204	204	204	204	204	204	204	204
Casing steel	4276	4288	4288	4276	4291	4296	4293	4294	4309	4291
Mk. 44 auxiliary detonator	213	212	213	213	212	214	212	214	215	213
Booster weight	25	25	25	25	25	25	25	25	25	25
Mk. 45 fuze	748	752	753	748	749	749	751	742	748	754
Metal parts, fuze + aux. det.	862	864	866	861	861	863	862	856	863	867
General recovery data:										
Casing steel fragments***	4331	4356	4343	4291	4302	4269	4274	4314	4324	4350
Weight of fragments>1 gram	4179	4230	4243	4170	4174	4085	4063	4101	4129	4092
Copper fragments from rotating band	200	202	200	206	202	196	196	201	194	193
Fuze and aux. det. fragments	842	810	845	826	812	826	810	815	796	809

*Charge weights and empty casing weights as given by MAD, Fort Mifflin.

**Nominal value; casing steel weights may be in error by several grams due to variations in this quantity.

***May include a few small fragments from fuze or auxiliary detonator, not identifiable as such.

Table XI (Continued)

	TNT					Composition A-3				
	#56	#63	#64	#65	#69	#57	#66	#67	#68	#72
Detailed recovery data:										
Casing steel fragments										
No. with mass:	361-400 g.									
	324-361									
	289-324									
	256-289									
	225-256									
	196-225									
	169-196									
	144-169									
	121-144									
	100-121									
	81-100									
	64-81									
	49-64									
	36-49									
	25-36									
	16-25									
	9-16									
	4-9									
	1-4									
	0.25-1									
No. coarse nose fragments	7	6	6	7	7	9	8	8	9	8
Mass of coarse nose fragments	1598g.	1657g.	1629g.	1662g.	1736g.	1465g.	1606g.	1726g.	1757g.	1671g.
Average mass of fragments	10.84	11.43	14.52	11.05	10.37	7.80	7.25	6.99	7.88	7.14
>1 gram, excluding nose fragments										
M ₂ excluding nose fragments	1.77	1.84	2.15	1.80	1.72	1.41	1.34	1.30	1.42	1.32

Table XI (continued)

	TNT					Composition A-3				
	#56	#63	#64	#65	#69	#57	#66	#67	#68	#72
Detailed recovery data:										
Casing steel fragments										
Copper rotating band fragments										
No. with mass 0.1 - 16g.	68	48	56	68	80	81	83	94	76	97
Fuze and aux. det. fragments										
No. with mass > 500g.	0	1	1	1	1	0	1	1	1	1
400 - 500	1	0	0	0	0	1	0	0	0	0
No. with mass										
100 - 150	1	0	0	0	0	1	0	00	0	0
9 - 36	4	4	6	3	6	5	5	4	53	3
0.1 - 9	197	135	140	152	142	260	214	178	191	183

Table XII

Average cumulative numbers of steel casing fragments excluding massive nose fragments
-Mk. 31-1 3" A.A. projectile, Mk. 45 fuze with Mk. 44 auxiliary detonator

m_i (grains)	TNT			Composition A		
	N_i (av. obs., excluding #64)	N_i (calc., empirical exponential law)		N_i (av. obs.)	N_i (calc., empirical exponential law)	
		Difference $N_i(\text{obs.}) - N_i(\text{calc.})$	Difference $N_i(\text{obs.}) - N_i(\text{calc.})$		Difference $N_i(\text{obs.}) - N_i(\text{calc.})$	Difference $N_i(\text{obs.}) - N_i(\text{calc.})$
100	1.0	1.5	-0.5	0		
81	1.5	2.6	-1.1	0.2	0.9	-0.7
64	4.5 \pm 0.5	4.5	0.0	0.2	1.9	-1.7
49	9.5 \pm 1.3	8	+1.5	1.6	3.3	-1.7
36	15 \pm 0.5	14	+1	6.4 \pm 1.1	8.4	-2.0
25	22 \pm 2	24	-2	16 \pm 1.4	18	-2
16	41 \pm 1	43	2	37 \pm 2	37	0
9	75 \pm 8	75	0	86 \pm 3	76	+10
4	137 \pm 10	132	+5	167 \pm 2	159	+8
1	231 \pm 5	(231)	(0)	331 \pm 12	(331)	(0)
0.25	339 \pm 17	306	+33	545 \pm 20	477	+72

c) General summary for Composition A and TNT.

Table XIII presents a general summary for the TNT-loaded and the Composition A-loaded 3" A.A. projectiles, Mk. 27-3 and Mk. 31-1. One should note that only two Composition A-loaded Mk. 27-3 projectiles were fired. A further qualification is that of the shell listed in the table, only the Mk. 27-3 TNT-loaded shell initiated with Mk. 51 MT fuze were checked individually for physical properties (i.e., hardness), while the Mk. 27-3 Composition A loaded shell were actually from a different lot.

One cannot readily compare the distributions of the Mk. 27-3 with those of the Mk. 31-1 projectiles. As has been noted, the slow nose fragments produced by the latter projectiles (because of the inert VT fuze bodies) were readily distinguished from the other high-velocity casing fragments and could be treated separately. In the case of the Mk. 27-3 projectile, the removable fuze adapter was treated separately, but it was impossible to distinguish in any clear-cut manner between low-velocity nose fragments and those fragments beginning at the nose but extending far enough down the side-wall to partake of true side-wall properties, though it was undoubtedly true that fragmentation was generally coarser towards the nose than towards the base. Thus the values of M_0 given in Table XIII do not reflect accurately the relative coarseness of the casing distributions for Mk. 27-3 as compared with Mk. 31-1, since in the latter case, nose fragments were excluded, while in the former case, fragments from the corresponding part of the casing, which were finer, were included.

In comparing Composition A with TNT, one observes that the cumulative numbers of fragments down to 9 grams are about the same for the two explosives, Composition A showing a slight advantage. Down to 1 gram, however, the numbers for Composition A are 48%, 59% and 42% greater than for TNT in the shell Mk. 27-3 with Mk. 51 MT fuze, Mk. 31-1 with Mk. 58 VT fuze and Mk. 31-1 with Mk. 45 VT fuze, respectively. The average masses of the fragments having individual masses equal to or exceeding 1 gram is 52%, 60% and 47% greater for TNT than for Composition A in the three respective shell, massive nose fragments in the case of Mk. 31-1 being excluded.

The average side-wall fragment velocities at 9' from the shell, as determined by R.W. Drake at this laboratory (OSRD Reports Nos; 5266, 5267 and 5531) are as follows:

	<u>TNT</u>	<u>Composition A</u>
Mk. 27-3, Mk. 51 fuze	2060 ft/sec.	2530 ft/sec.
Mk. 27-3 (EX-2), Mk. 58 fuze*	1960	2360
Mk. 27-3 (EX-2), Mk. 45 fuze*	1710	2220

The velocities are thus between 20% and 30% greater for Composition A than for TNT. According to Motz's theoretical treatment (Equation 5), we should expect M_0 to be greater for TNT by about 15%. It is actually greater by 30-40%. These shells, with their relatively large fuze cavities, are of course not at all ideal in shape.

* For the Mk. 31-1 shell, the velocities are presumably about 3% greater, due to the slightly smaller casing thickness. H. N. Shapiro, in a recent report from The New Mexico Experimental range, has given an average velocity for Composition A in the Mk. 31-1 projectile with Mk. 58 VT fuze of 2780 ft/sec., averaged over the first thirty feet of flight. This value is for statically initiated shell and is appreciably higher than the value reported by Drake for the EX-2 shell. Several factors combined appear to account for the discrepancy. Upon examining Drake's fragments, it turns out that an unfortunately large proportion of all those passing by the illuminated slits and recorded by the rotating drum camera, happened to come from the region of the shell under the rotating band, where of course the overall casing thickness is greater than elsewhere. This fact, combined with the generally slightly heavier casing thickness of the EX-2 shell, resulted in slower original velocities for Drake's fragments. In addition, fragment retardation at the New Mexico range is significantly smaller because of the higher altitude.

Summary of fragment mass distribution data for 3" A.A. projectiles, TNT and Composition A-3

* Massive nose fragments excluded in computing this quantity.

** Based on only two shots, showing rather wide divergence in this range. Observed numbers, 706 and 576.

One should note in general that for the Mk. 27-3 projectiles, the fuze adapters have not been included. The Mk. 31-1 projectiles are threaded directly to receive the VT fuzes, without separate adapters. Average casing steel mass for Mk. 27-3 = 3915 g., for Mk. 31-1 = 4290 g.

Appendix I

Chi-square test for goodness-of-fit of the exponential law.

We are indebted to Dr. Henry Scheffé of Division 2, NDRC for suggesting this test and for much helpful information generally concerning the statistical treatment of shell fragment distribution data.

We wish to test the hypothesis that the observed set of numbers N_{ij} of fragments within the various mass groups $M_1 < m^{1/2} < M_j$ constitute a random sample from some exponential distribution with probability density function:

$$\begin{aligned} f(M) &= (1/M_0) \exp \left(- \frac{M - M_1}{M_0} \right) & \text{if } M \geq M_1 \\ &= 0 & \text{if } M < M_1 \end{aligned}$$

where $M = m^{1/2}$. We are excluding from consideration fragments with individual masses below some lower limit m_1 , taken in the present application (to 3" shell) as 1 (gram).

Having determined an estimated value of M_0 (say M_0^*) by Equation (11) and derived therefrom by Equation (11') a value of $AM_0 = (AM_0)^*$ making use of the total number N_1 of fragments with individual masses equal to or greater than the limit m_1 (= 1 gram), we divide the data for convenience into eight classes: the seven classes $i < M < i+1$ for $i = 1, 2, \dots, 7$ and the class $M \geq 8$. The estimated value M_0^* is not necessarily equal to the "true" value of M_0 for the supposed distribution of which we may have a sample, but it will serve for purposes of calculation.

For each class, a theoretical number N_{ij}' is calculated from the formula:

$$N_{ij}' = (AM_0)^* \left[\exp(-i/M_0^*) - \exp(-\frac{i+1}{M_0^*}) \right]$$

for $i = 1, 2, \dots, 7$ and

$$N_8' = (AM_0)^* \exp(-8/M_0^*)$$

Shell #75: $M_0^* = 2.03$

$(AM_0)^* = 466$

$N_1 = 284$

i	$\exp(-i/M_0^*)$	$(AM_0)^* \exp(-i/M_0^*)$	N_{ij}	N_{ij}	$\Delta i x^2$
1	0.610	284.0	110.4	108	0.05
2	0.373	173.6	69.8	68	0.05
3	0.223	103.8	39.1	53	4.93
4	0.139	64.7	25.1	20	1.04
5	0.085	39.6	15.4	10	1.89
6	0.052	24.2	9.3	6	1.17
7	0.032	14.9	6.1	6	0.00
8	0.019	8.8	8.8	13	<u>2.00</u>

$x^2 = 11.13$

Appendix II

Application of the method of maximum likelihood to the estimation of the parameter M_0 in the Mott distribution law.

This method is a modification of one suggested to us informally by Dr. L. H. Thomas of the Ballistic Research Laboratory. Let a_{ij} denote the probability according to the assumed distribution law that a fragment will have a mass m in the range $M_i < m^{1/2} < M_j$. Then the probability P of obtaining any given distribution, specified by the numbers N_{ij} in the various classes M_1 to M_2 , M_2 to M_3 , . . . , M_1 to M_j , etc. is:

$$P = N! \prod \frac{(a_{ij})^{N_{ij}}}{N_{ij}!}$$

or:

$$\ln P = \log N! + \sum (N_{ij} \ln a_{ij} - \ln N_{ij}!)$$

summed over all classes, N being the total number. This statement involves the assumption that the probability of finding a given fragment in a particular class is independent of the distribution of the other fragments. While this situation is not physically true, we may assume that it is practically so due to the complex nature of the break-up process.

We assume that all fragments down to some least individual fragment mass m_1 , numbering N_1 , are distributed according to the Mott equation and ignore all smaller fragments. Of the number counted, the fraction:

$$\frac{N_{ij}'}{N_1} = \frac{\exp(-M_i/M_0) - \exp(-M_j/M_0)}{\exp(-M_i/M_0)}$$

therefore represents the ideal fraction in the range $M_i < m^{1/2} < M_j$.

This fraction is taken as representing the probability a_{ij} .

Let us now vary the parameter M_0 so as to make the probability of the observed distribution a maximum:

$$\frac{d \ln P}{dM_0} = \sum \frac{N_{ij}}{a_{ij}} \frac{da_{ij}}{dM_0} = 0$$

Carrying out the differentiation with

$$a_{ij} = \frac{\exp(-M_i/M_0) - \exp(-M_j/M_0)}{\exp(-M_1/M_0) - \exp(-M_j/M_0)}$$

we obtain:

$$\sum N_{ij} \frac{M_i \exp(-M_i/M_0) - M_j \exp(-M_j/M_0)}{\exp(-M_i/M_0) - \exp(-M_j/M_0)} - \sum N_{ij} M_1 = 0$$

$$\text{or: } \sum N_{ij} \frac{M_i \exp\left(\frac{M_j - M_i}{M_0}\right) - M_j}{\exp\left(\frac{M_j - M_i}{M_0}\right) - 1} = M_1 N_1$$

This equation is quite general with respect to the choice of class limits M_i and M_j and could be solved by successive approximations to find the value of M_0 that gives the observed distribution maximum likelihood as compared with all other possible values of M_0 . The equation is greatly simplified however by suitable choice of these limits. Thus, adopting the conventions: $M_1 = 1$ and $M_j = M_i + 1$ (i.e., the classes 1 - 4 grams, 4 - 9 grams, 9 - 16 grams, etc.), we obtain:

$$\exp\left(\frac{1}{M_0}\right) = \frac{\sum i N_{ij}}{\sum i N_{ij} - N_1}$$

$$\text{or } \frac{0.4343}{M_0} = \log_{10} \frac{\sum i N_{ij}}{\sum i N_{ij} - N_1}$$

where the sum $\sum iN_{ij}$ extends over $i = 1, 2, 3, \dots$ to the highest value of i (i.e., of M_i) required to include the heaviest fragments.

The following table shows the application of this method of estimating M_0 to the data for Shell #75 in Table II (Mk.27-3 3" A.A. projectile loaded with cast TNT):

Shell #75

m	i	N_{ij}	iN_{ij}
1 - 4 grams	1	108	108
4 - 9	2	63	136
9 - 16	3	53	159
16 - 25	4	20	80
25 - 36	5	10	50
36 - 49	6	6	36
49 - 64	7	6	42
64 - 81	8	4	32
81 - 100	9	6	54
100 - 121	10	2	20
121 - 144	11	1	11

$$N_i = 284 \quad \sum iN_{ij} = 728$$

$$\frac{0.4343}{M_0} = \log \frac{728}{444}$$

$$= 0.2147$$

$$M_0 = 2.023$$

Like the method of averaging described in the text of this report (Equation 11), this method will give a formal value of M_0 whether or not the distribution actually is consistent with the exponential law. If the observed distribution does not satisfy the law (using as criterion the Chi-square test described in Appendix I, in which the M_0^* value estimated by the method of maximum likelihood may be introduced to calculate the N_{ij}'), the method of maximum likelihood is not legitimate and the formal value of M_0 is meaningless.

Plate 3

Shot No.75 - Mk. 27-3 3" A.A. Projectile with Mk. 51
MT Fuze and Mk. 54 Auxiliary Detonator,
Cast TNT. Steel casing fragments arranged
according to mass.



SHOT # 70
 MARK 21-3
 3" A.A. Projectile
 365g Cast TNT
 MARK 51 Fuzo



121-M-149 100-M-121 31-M-100 64-M-819



49-M-649 36-M-49 28-M-36



16-M-25



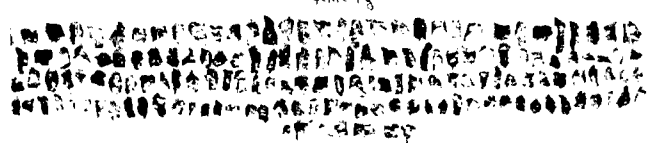
9-M-16



4-M-9



1-M-4



4-M-29



Copper Jacketing Band



21-M-149



4-M-29



Plate 4

Shot No. 75. - Fragments of Plate 3 arranged approximately according to regions of shell from which they came. No attempt made to order fragments having masses less than 1 gram.

SRot H 75

MARK 21-3

3" A A Projectile

365g Chit INI

Miner si fuge

PLANT
PLANT



PLANT
PLANT

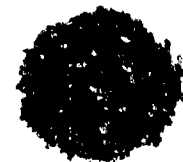
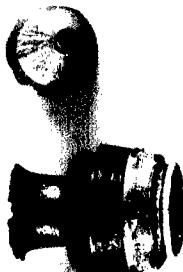
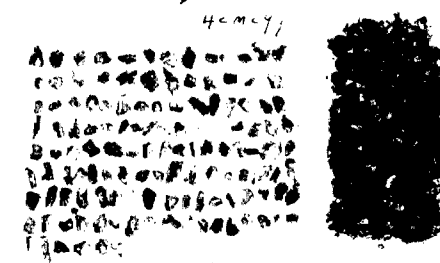
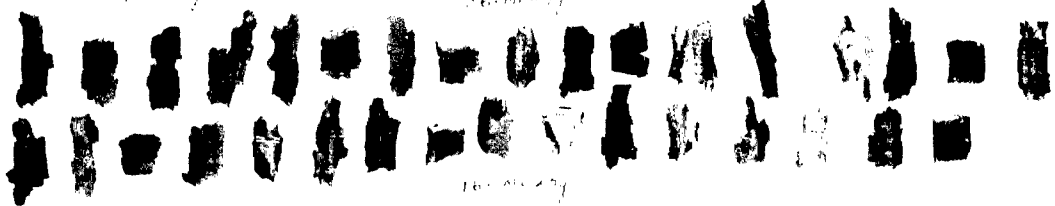
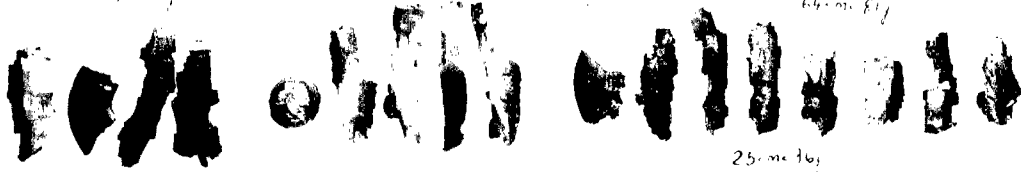
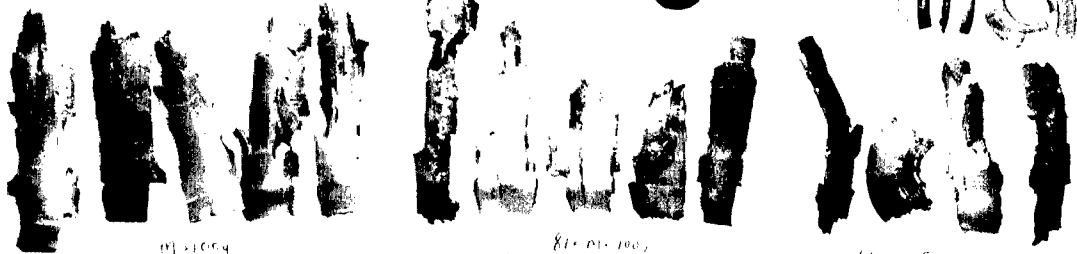
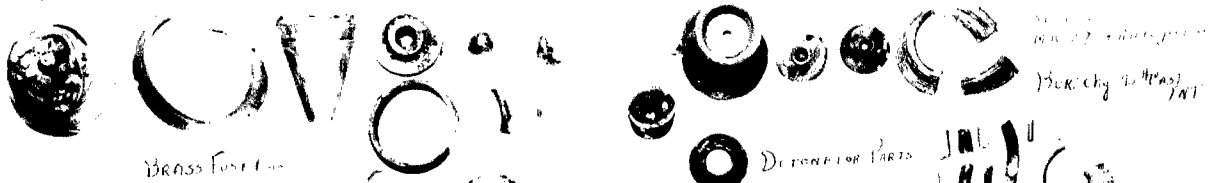


Plate 5

Shot No. 21 - Mk. 27-3 3" A.A. Projectile with Mk. 51-2
MT Fuze and Mk. 46 Auxiliary Detonator,
Cast TNT.



COPPER ROTATING BAND

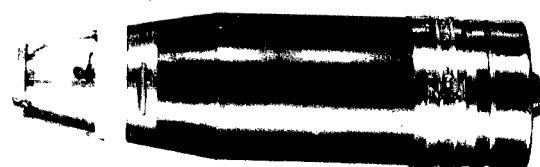
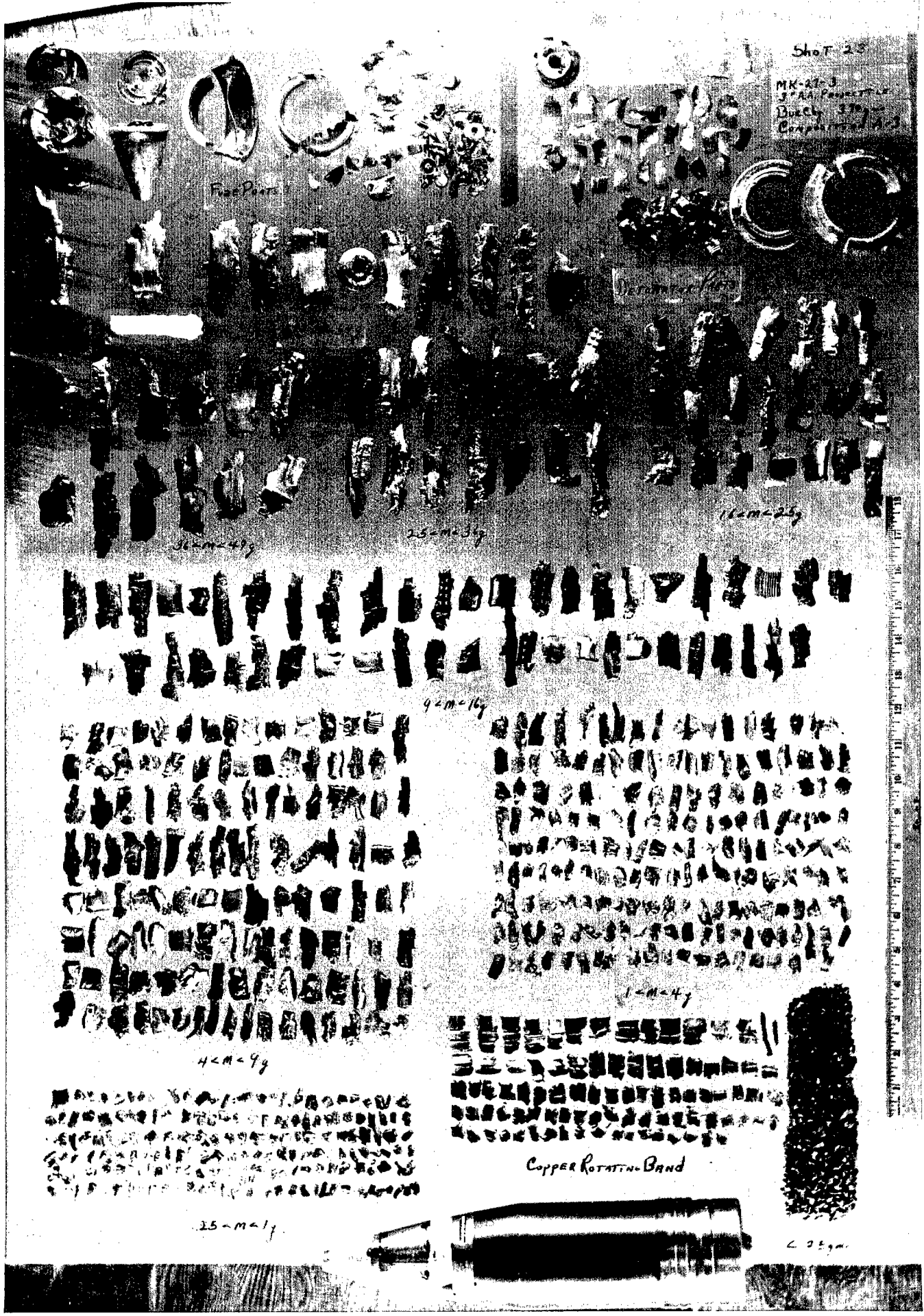


Plate 6

Shot No. 23 - Mk. 27-3 3" A.A. Projectile with Mk. 51-2
MT Fuze and Mk. 46 Auxiliary Detonator,
Pressed Composition A-3.

Shot 25

MK-42-3
3" AA Projectile
Buach 375
Compressed Air



Free Port

25-m-34

11-m-24

9-m-16

4-m-9

1-m-4

25-m-1

Copper Rotatin. Band

25-m-1

1

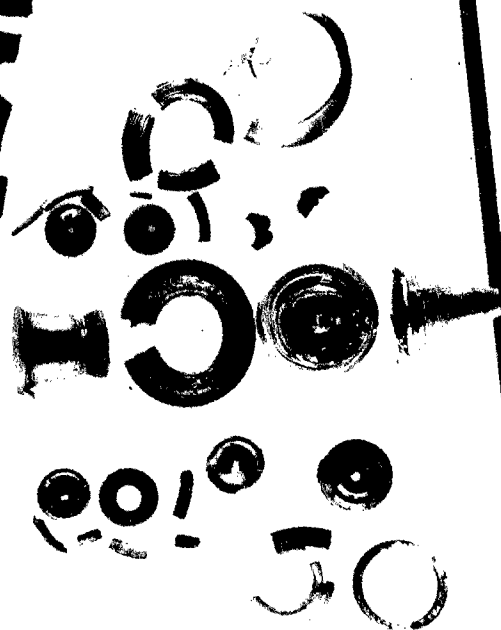
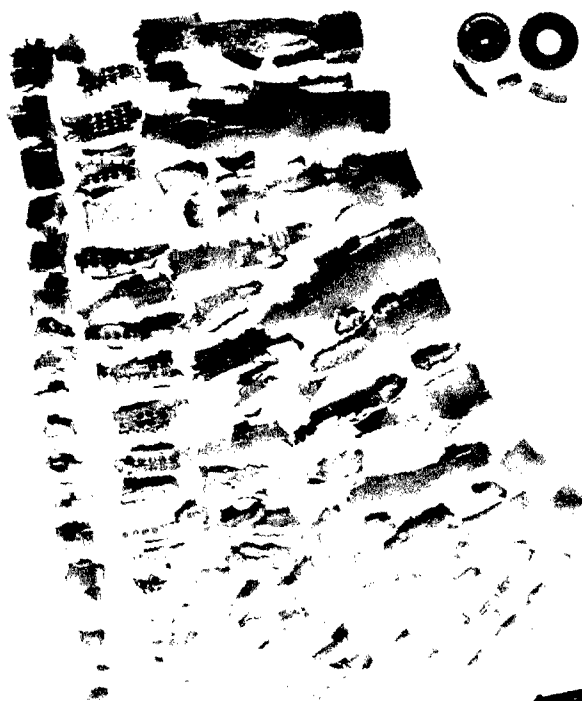
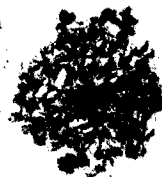


Plate 8

Shot No. 23 - Fragments of Plate 6 (Composition A-3)
rearranged to show origins.

CONFIDENTIAL

Shot 23

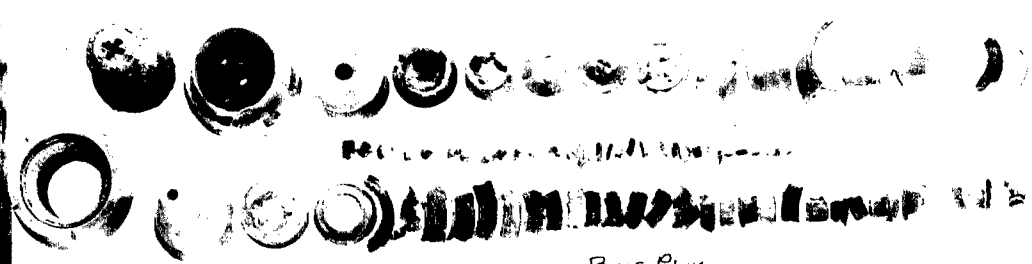
MK-27-3
3" A.A. Projectile
Burchn. 370 gms
Composition A-3



Plate 9

Shot No. 58 - Mk. 27-3 3" A.A. Projectile with Mk. 51
MT Fuze and Mk. 54 Auxiliary Detonator,
Pressed 50-50 Potassium Nitrate/ Composition A.

Shot # 58
MARK 27-3
3" AA PROJECTILE
400 gr. 70 Comp A/KNO₃



BASE PLUG

ADAPTER



81 cm 100g

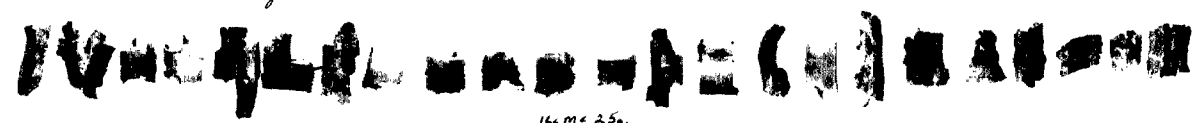
64 cm 81g

49 cm 64g

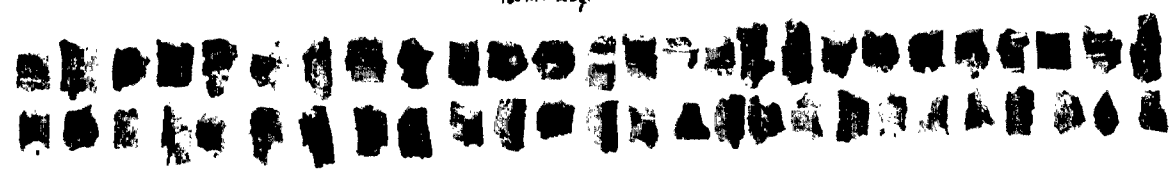


36 cm 49g

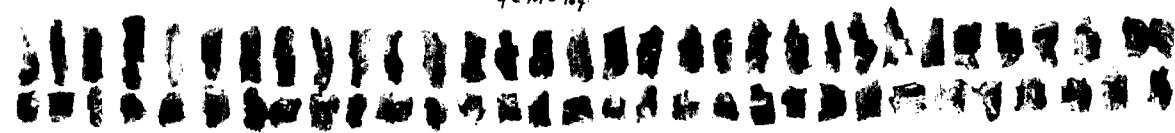
25 cm 36g



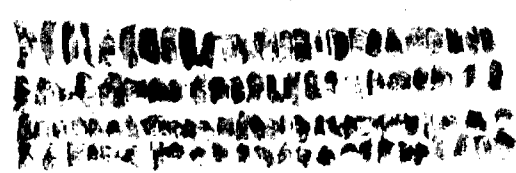
16 cm 25g



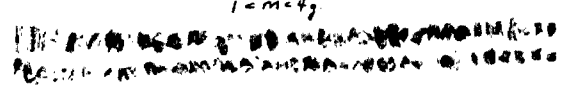
9 cm 16g



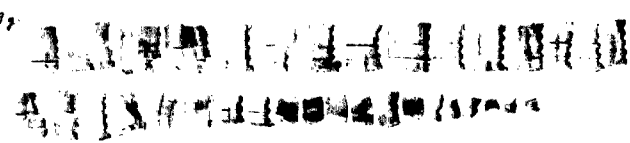
4 cm 9g



1 cm 4g



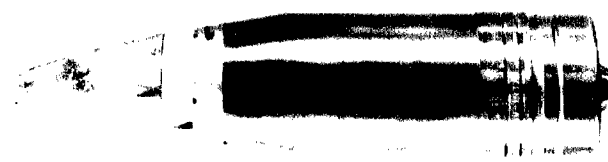
225 cm 1g



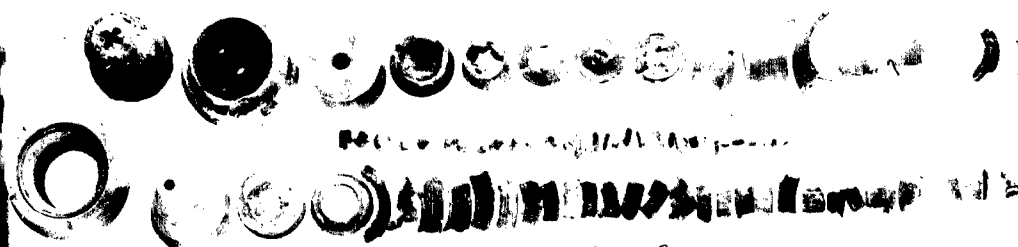
COPPER ROTATING BAND



20 25g



Shot #58
MARK 27-3
3" AA PROJECTILE
40% Comp A/KNO₃



BASE PLUG

ADAPTER



81mc 100g

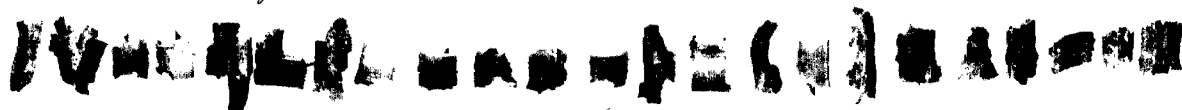
64mc 81g

49mc 64g

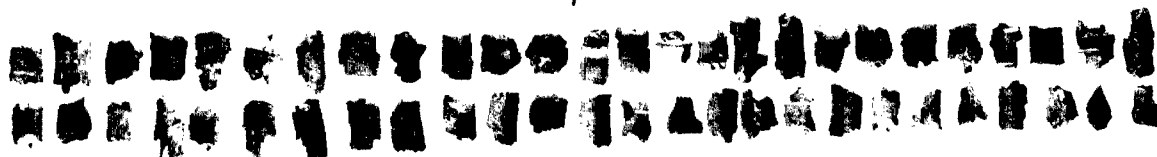


36mc 49g

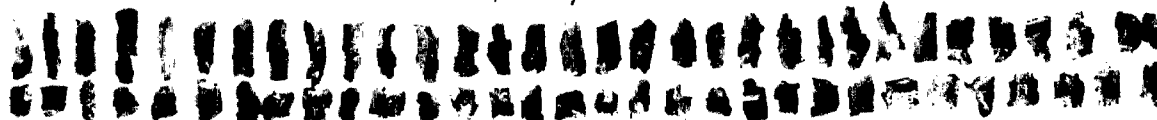
25mc 36g



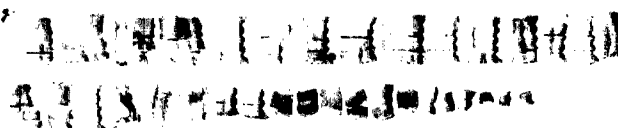
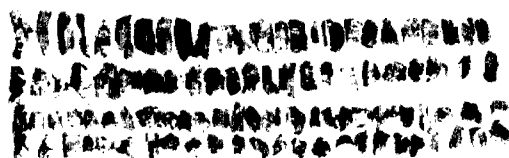
16mc 25g



9mc 16g



4mc 9g



COPPER ROTATING BAND

1mc 4g



225mc 1g



20.25g



Plate 10

Shot No. 58 - Fragments of Plate 9 (50-50 Potassium Nitrate/ Composition A) rearranged to show origins.

Sheet 11 of 12
Date 1/1/57
3" AA Project
400gms. 1/2" Comp A/RHC

10-10-56
11-11-56
12-12-56
13-13-56
14-14-56
15-15-56
16-16-56
17-17-56
18-18-56
19-19-56
20-20-56
21-21-56
22-22-56
23-23-56
24-24-56
25-25-56
26-26-56
27-27-56
28-28-56
29-29-56
30-30-56
31-31-56
32-32-56
33-33-56
34-34-56
35-35-56
36-36-56
37-37-56
38-38-56
39-39-56
40-40-56
41-41-56
42-42-56
43-43-56
44-44-56
45-45-56
46-46-56
47-47-56
48-48-56
49-49-56
50-50-56
51-51-56
52-52-56
53-53-56
54-54-56
55-55-56
56-56-56
57-57-56
58-58-56
59-59-56
60-60-56
61-61-56
62-62-56
63-63-56
64-64-56
65-65-56
66-66-56
67-67-56
68-68-56
69-69-56
70-70-56
71-71-56
72-72-56
73-73-56
74-74-56
75-75-56
76-76-56
77-77-56
78-78-56
79-79-56
80-80-56
81-81-56
82-82-56
83-83-56
84-84-56
85-85-56
86-86-56
87-87-56
88-88-56
89-89-56
90-90-56
91-91-56
92-92-56
93-93-56
94-94-56
95-95-56
96-96-56
97-97-56
98-98-56
99-99-56
100-100-56

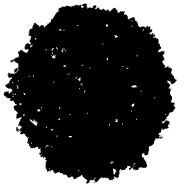
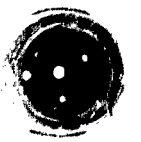
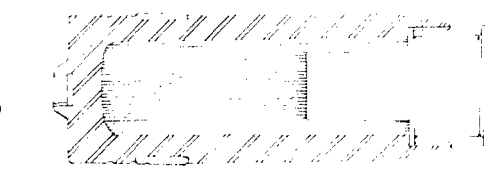
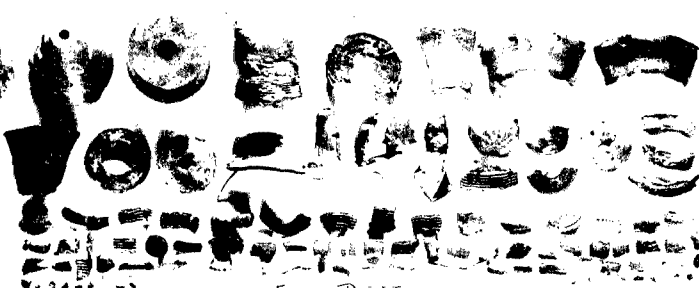


Plate 11

Shot No. 61 - Mk. 27-3 3" A.A. Projectile with Mk. 51 MT
Fuze and Mk. 54 Auxiliary Detonator,
Pressed 73-18-9 RDX/Aluminum/Wax.



Adapter



Fuze Parts

Shot # 61

Mark 27-3

3" A.A. Projectile

381g Aluminum Pump A

Mark 27-3



389-Mc327



91-M-108



64-M-81g



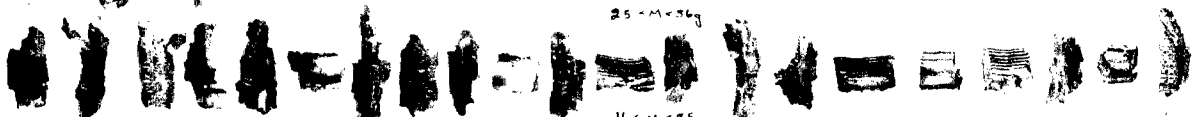
99-M-64g



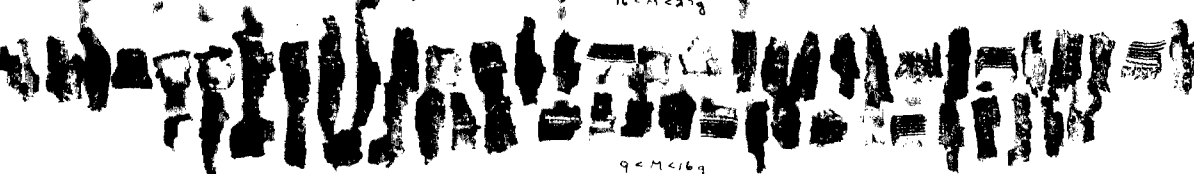
36-M-49g



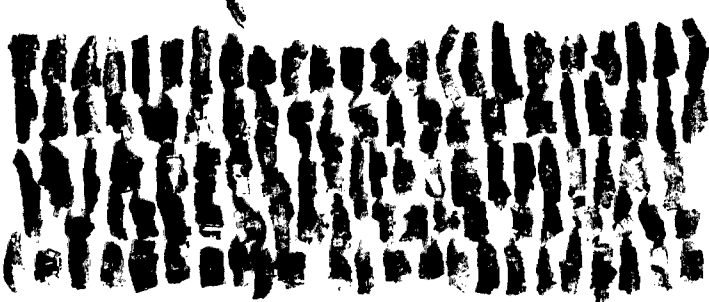
25-M-36g



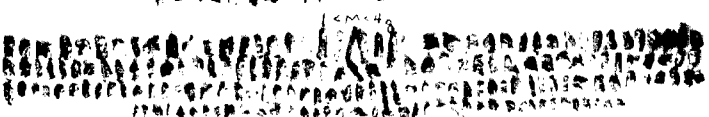
16-M-35g



9-M-16g



4-M-29



0.000000



Copper Rotating Band



2025



Plate 12

Shot No. 61 - Fragments of Plate 11 (Aluminized
Composition A) rearranged to show origins.

SHOT # 61

Mark 27-3

3" A. Projectile

121 g Aluminum Comp A

Mark 21 Forge

121 g Aluminum Comp A
Mark 21 Forge

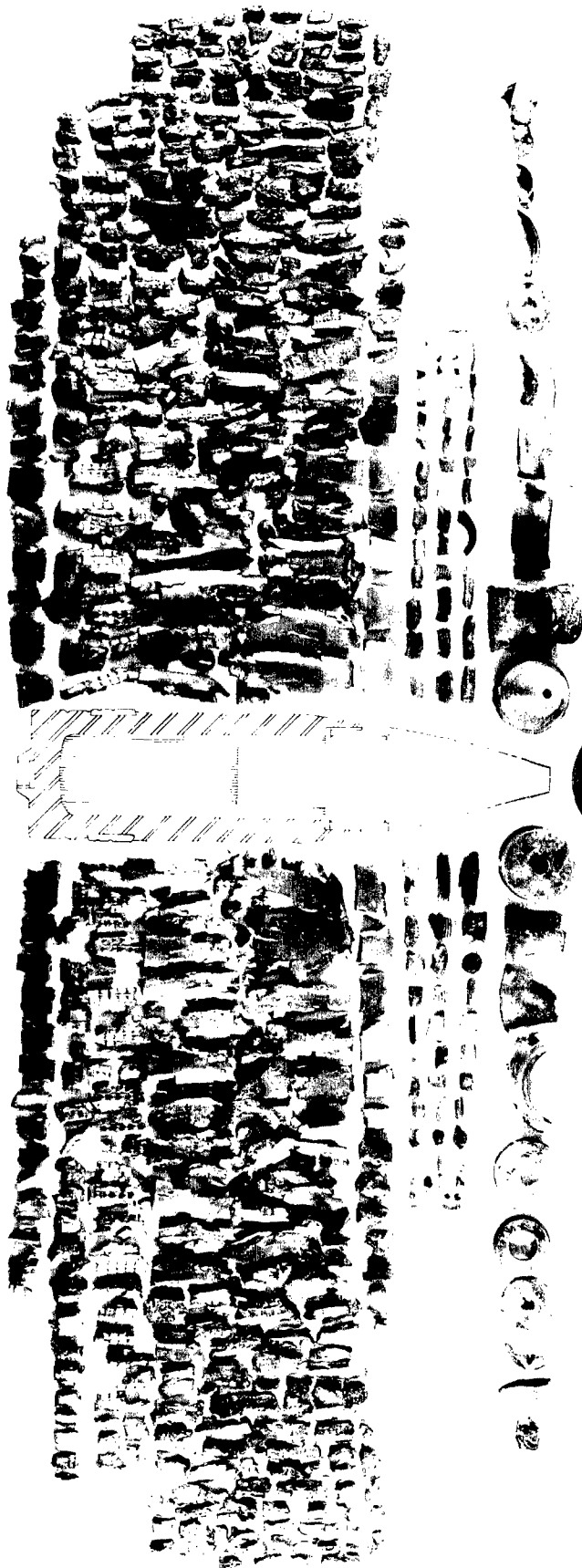


Plate 13

Shot No. 30 - Mk. 27-3 3" A.A. Projectile with 25 gram
Tetryl Booster and Brass End-plug, cast TNT.

Shot #3

Mark 27-3

3" A.A. Projectiles

Bur. Chg. 435g
Cast F.M.I.

"Tiny Tim"

Plug

Union

81-M-100

49-M-64

36-M-49

25-M-36

6-M-20

4-M-16

4-M-9

1-M-4

025-M-1

Copper Rotating Band

COAT

Plate 14

Shot No. 40 - Mk. 27-3 3" A.A. Projectile with 25 gram
Tetryl Booster and Brass End-plug, Cast
TNT-D2.



PLug

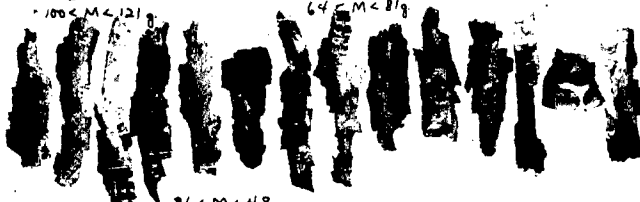


Adaptor Parts

SH-1
Mark-27-1
3" AA Projectile
Bur. Chg. 422 gm
Cast TNT D-2

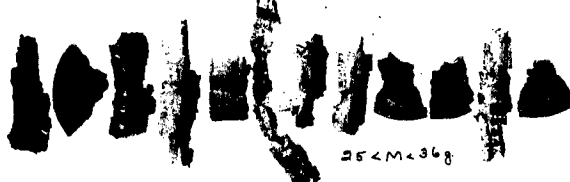


49 M < 64 g



100 M < 121

64 M < 81 g

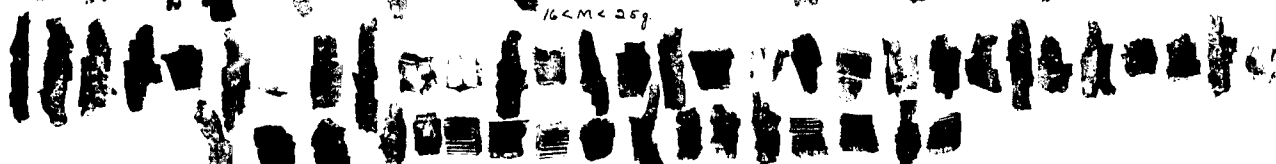


25 M < 36 g



36 M < 49 g

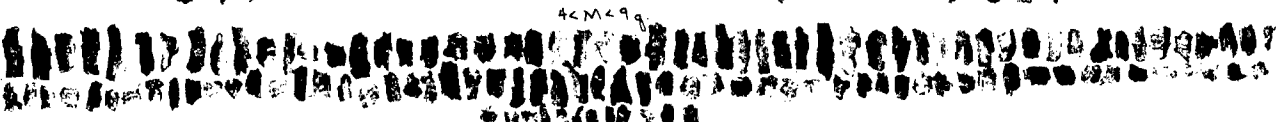
16 M < 25 g



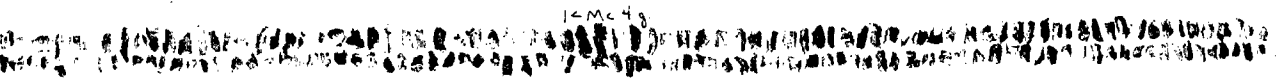
9 M < 16 g



4 M < 9 g



1 M < 4 g



0.25 M < 1 g



< 0.25 g



Copper Rotating Band

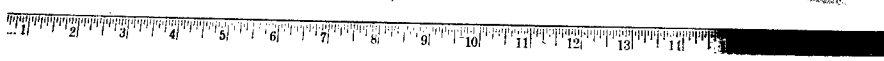
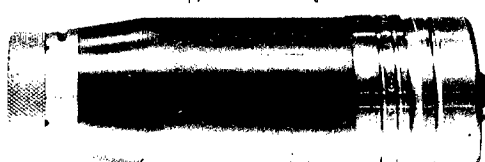


Plate 15

Shot No. 41 - Mk. 27-3 3" A.A. Projectile with 25 gram
Tetryl Booster and Brass End-plug, Cast
Picratol.



PLug



Adapter Parts

SHOT #41

MARK 27-3

3 AA Projectile

Bur Ctg 43491

Cast Ammonia Percolol



100 < M < 121g

81 < M < 100g

64 < M < 81g

49 < M < 64g

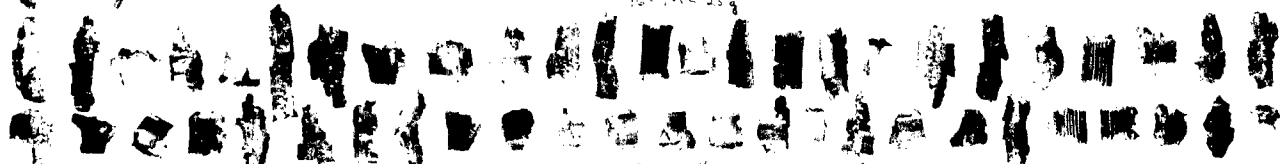


32 < M < 49g

25 < M < 32g



16 < M < 25g



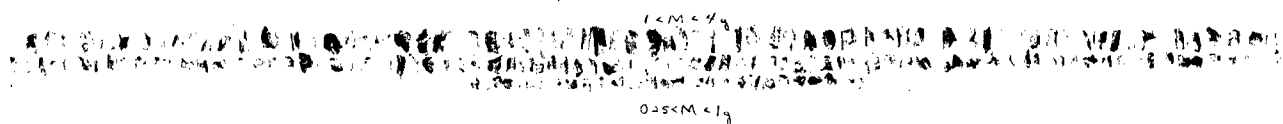
9 < M < 16g



4 < M < 9g



1 < M < 4g



0.25 < M < 1g



0.025g



Copper Rotating Band

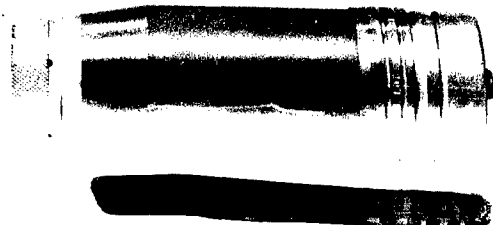
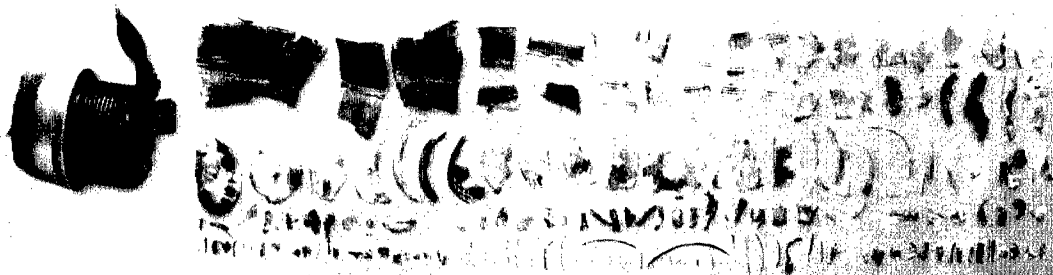


Plate 16

Shot No. 54 - Mk. 31-1 3" A.A. Projectile with Mk. 58 VT
Fuze and Mk. 44 Auxiliary Detonator, Cast TNT.



Shot # 54
 Mark 31-1
 3" AA Projectile
 ADJ East 100
 Mark 31-1



225-11-264

165-11-186

115-11-264

115-11-264

115-11-264



47-11-64

56-11-44



35-11-36

115-11-264



9-11-64



4-11-74

1. The first fragment is a small, dark, irregular fragment, possibly shrapnel or debris, arranged horizontally.

2. The second fragment is a small, dark, irregular fragment, possibly shrapnel or debris, arranged horizontally.

Copper Rivet Band



10-11-74

3. The third fragment is a small, dark, irregular fragment, possibly shrapnel or debris, arranged horizontally.

025-11-14

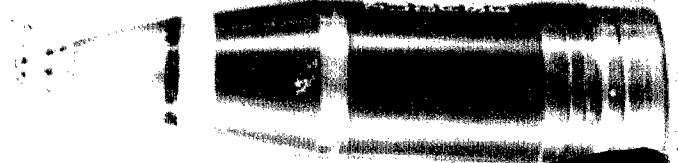


Plate 17

Shot No. 51 - Mk. 31-1 3" A.A. Projectile with Mk. 58 VT.
Fuze and Mk. 44 Auxiliary Detonator,
Pressed Composition A-3.

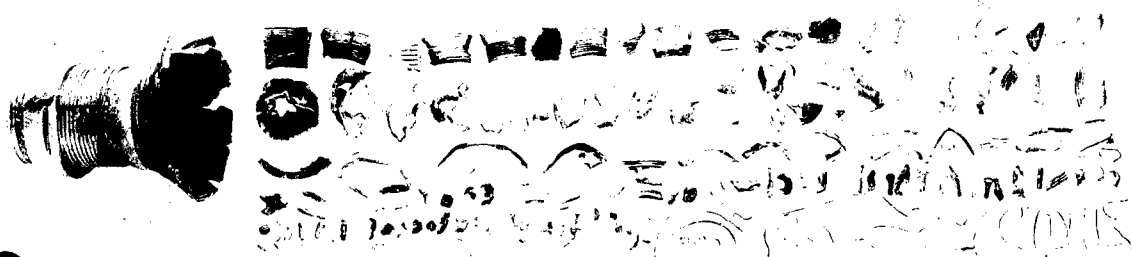
SP-1 # 51

Mark 31-1

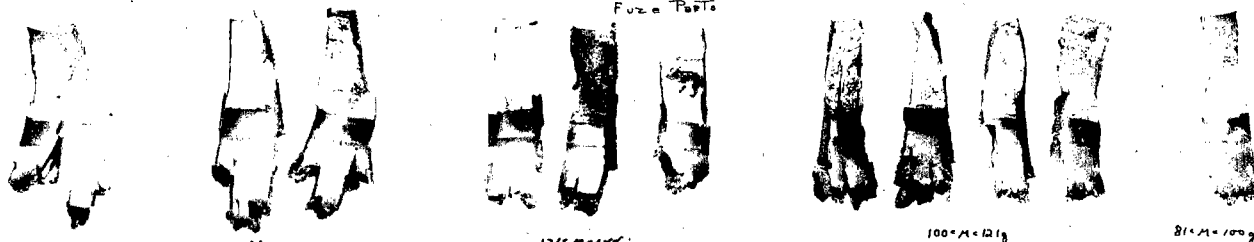
3" AA Projectile

281g Comp-A-3

Mark 52 Fuse



Fuze Parts



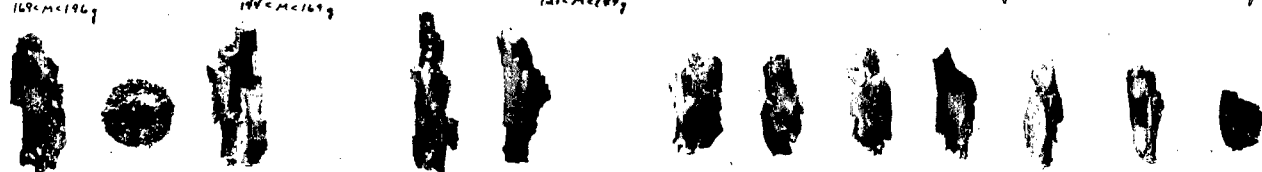
169-M-196

188-M-169

121-M-169

100-M-121

31-M-100



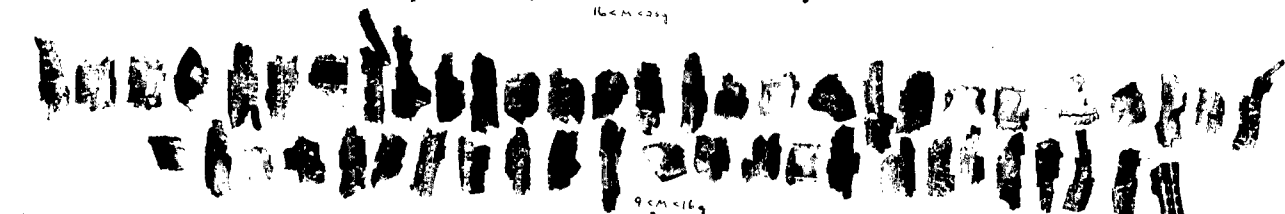
49-M-169

36-M-169

88-M-169



16-M-169



9-M-169



1-M-169



Copper Rotating Band



200g



0-M-169

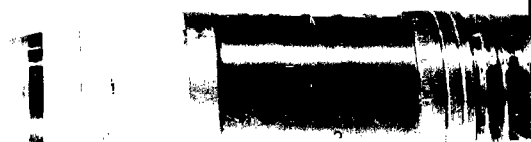
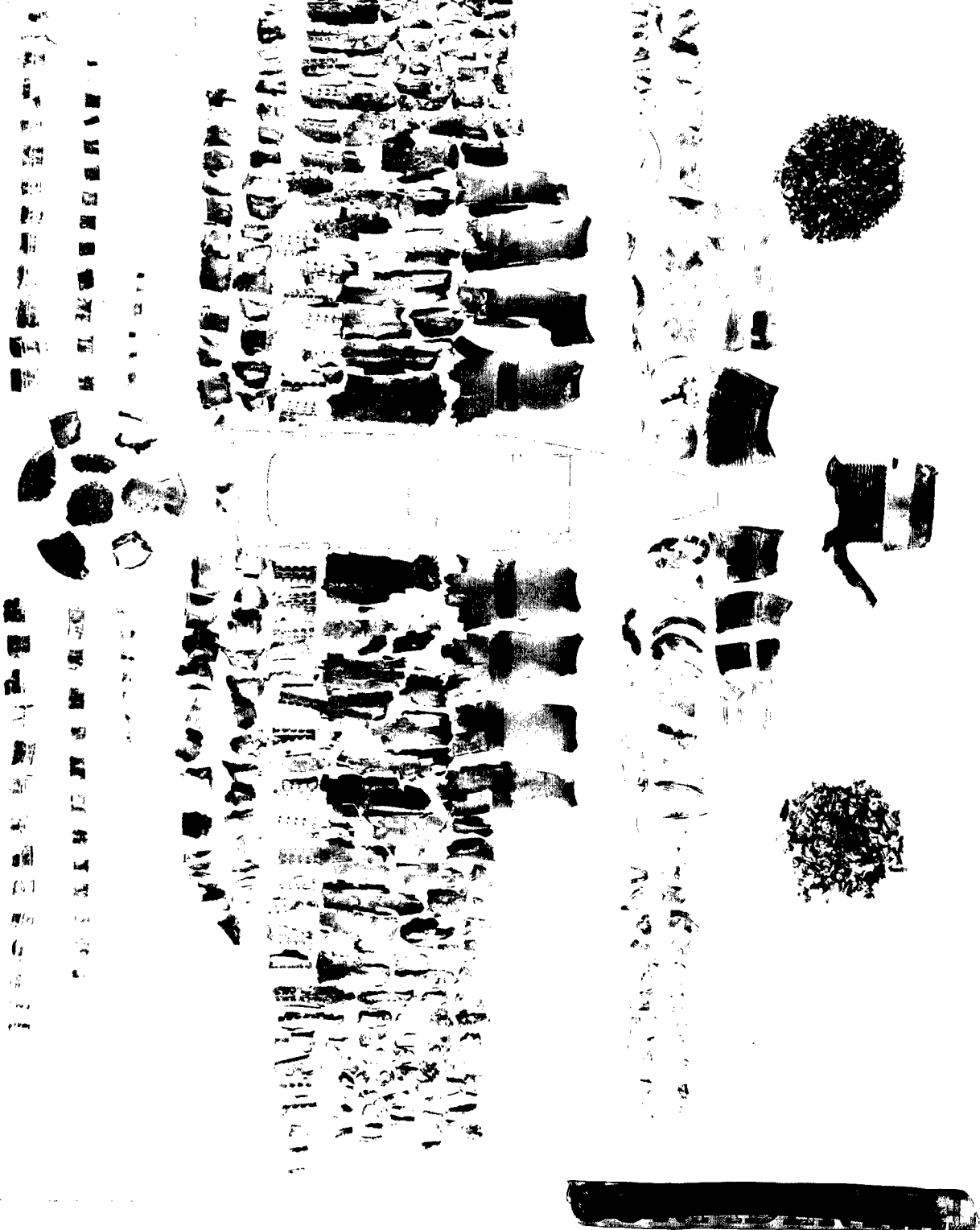


Plate 18

Shot No. 54 - Fragments of Plate 16 (TNT rearranged to
show origins.

Mark 58 FuzE





 UNCLASSIFIED

Plate 19

Shot No. 51 - Fragments of Plate 17 (Composition A-3)
rearranged to show origins.

 UNCLASSIFIED

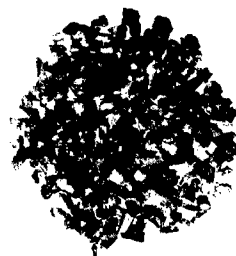
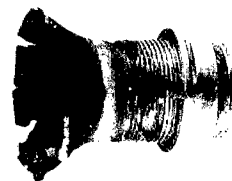
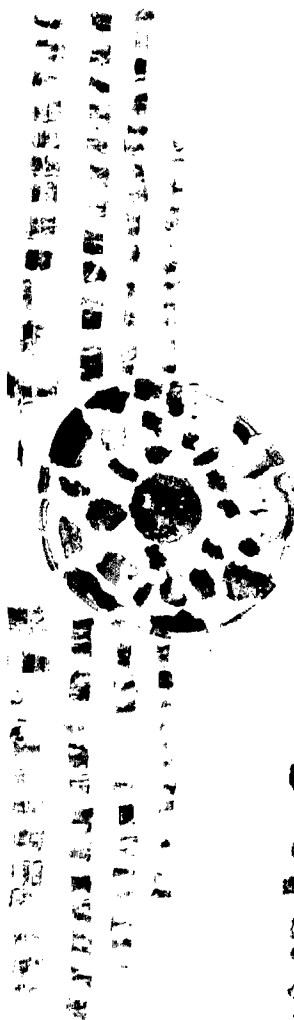
S.P.O. # 51

Mark 31-1

3" AA Projectile

291 g Comp A-1

Mark 58 Fuse

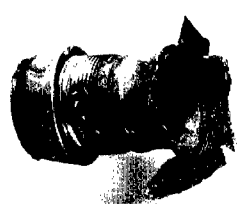


DECLASSIFIED

Plate 20

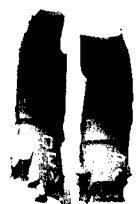
Shot No. 69 - Mk. 31-1 3" A.A. Projectile with Mk. 45
VT Fuze and Mk. 44 Auxiliary Detonator,
Cast TNT.

DECLASSIFIED
15 JAN 1983



SROF 8-69
MARK 31-1
3" A Projectile
227g Cast TNT
Mark 45 Fuse

Fuse Parts

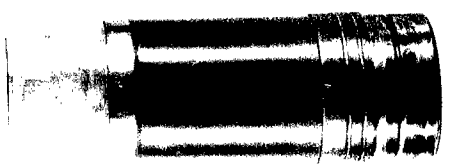
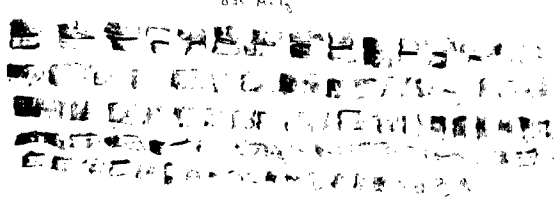
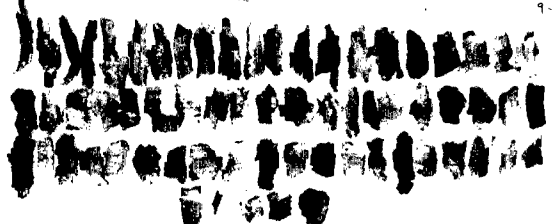
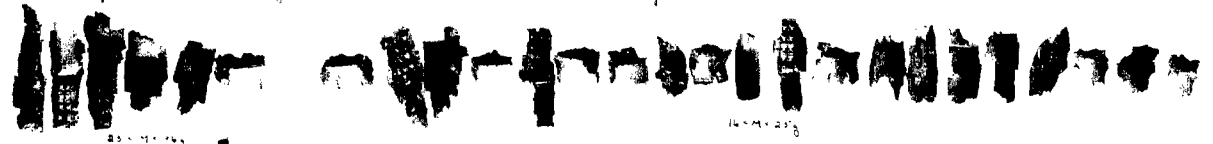


31-M-100g

67-M-81g

49-M-60g

36-M-49g

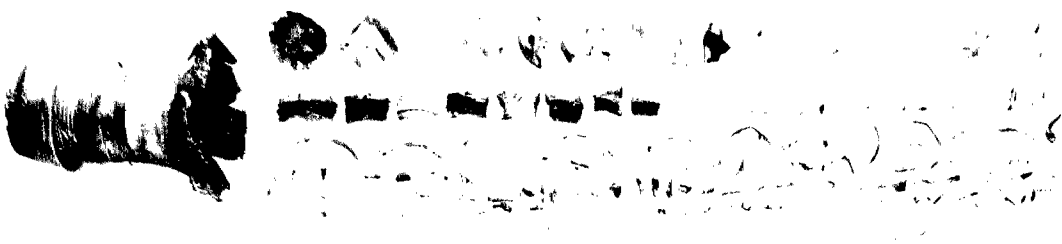


RECEIVED
JAN 10 1945

Plate 21

Shot No. 68 - Mk. 31-1 3" A.A. Projectile with Mk. 45
VT Fuze and Mk. 44 Auxiliary Detonator,
Pressed Composition A-3.

5/21/1964
Mark 111
3" x 4" Tag 111
240g Pressed Comp A
Mark 111 Tag



Tag 111



225 x 111-225g



175 x 111-225g



175 x 111-225g



175 x 111-225g



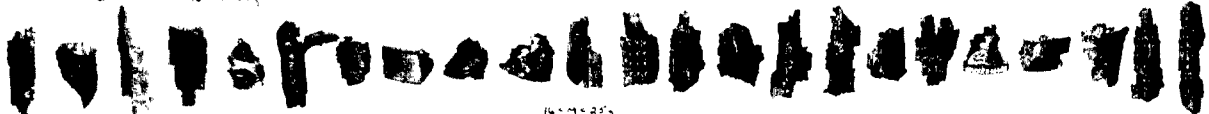
175 x 111-225g



175 x 111-225g



175 x 111-225g



175 x 111-225g



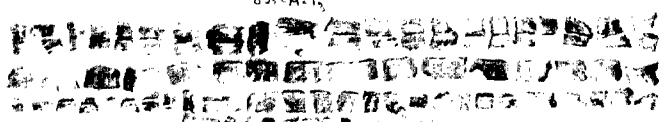
175 x 111-225g



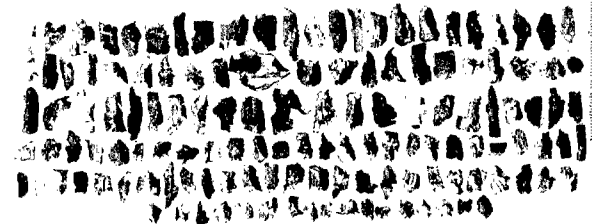
175 x 111-225g



175 x 111-225g



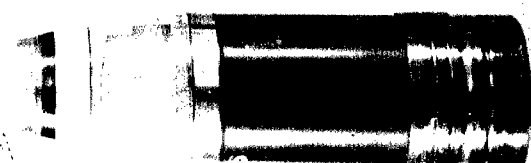
175 x 111-225g



175 x 111-225g



175 x 111-225g



UNCLASSIFIED

Plate 22

Shot No. 69 - Fragments of Plate 20 (TNT) rearranged to show origins.

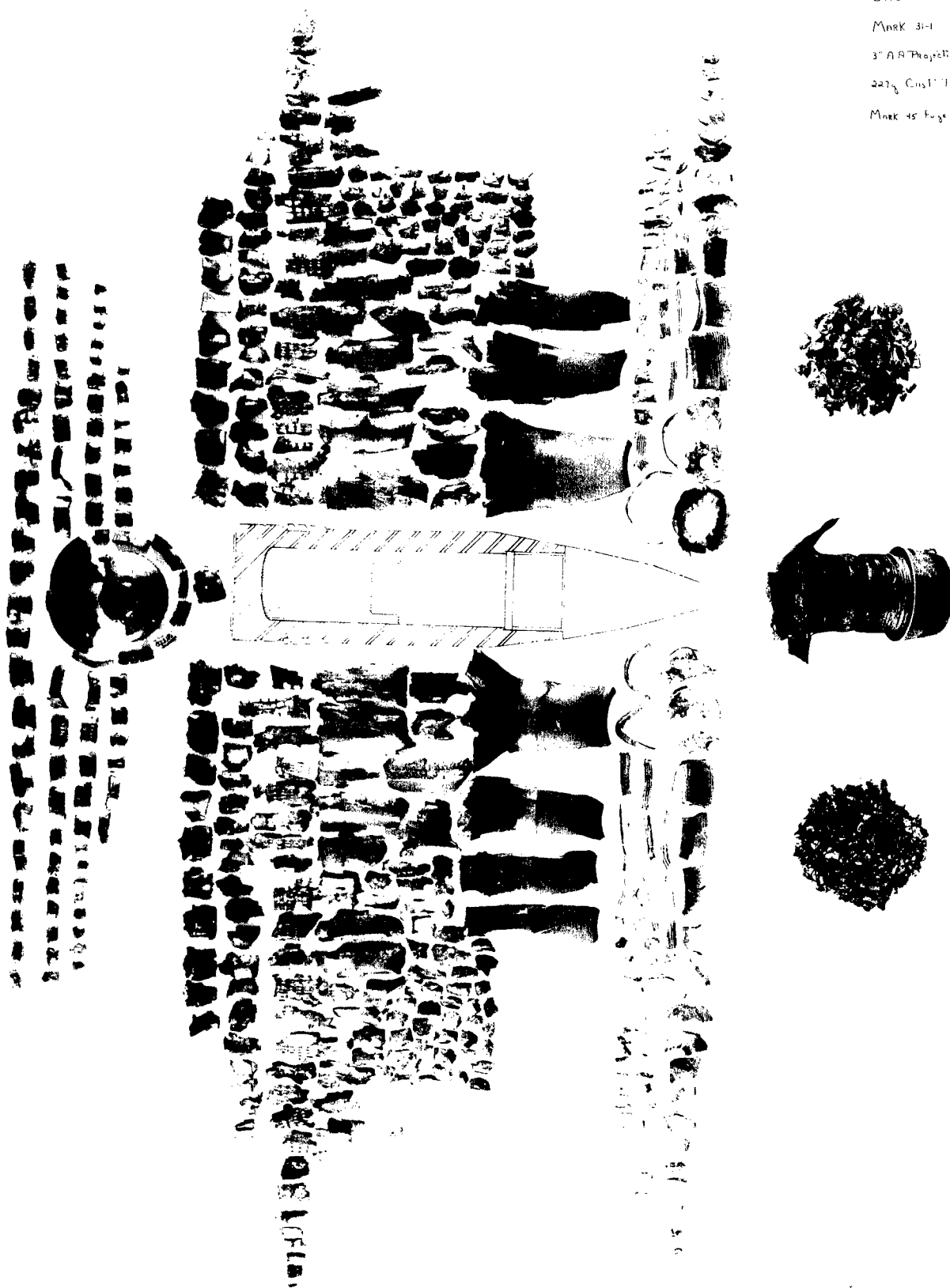
Shot # 49

Mark 31-1

3" AA Projectile

227g Cast TNT

Mark 45 Fuse

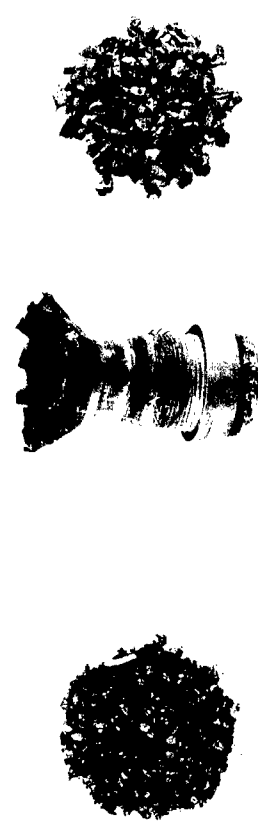
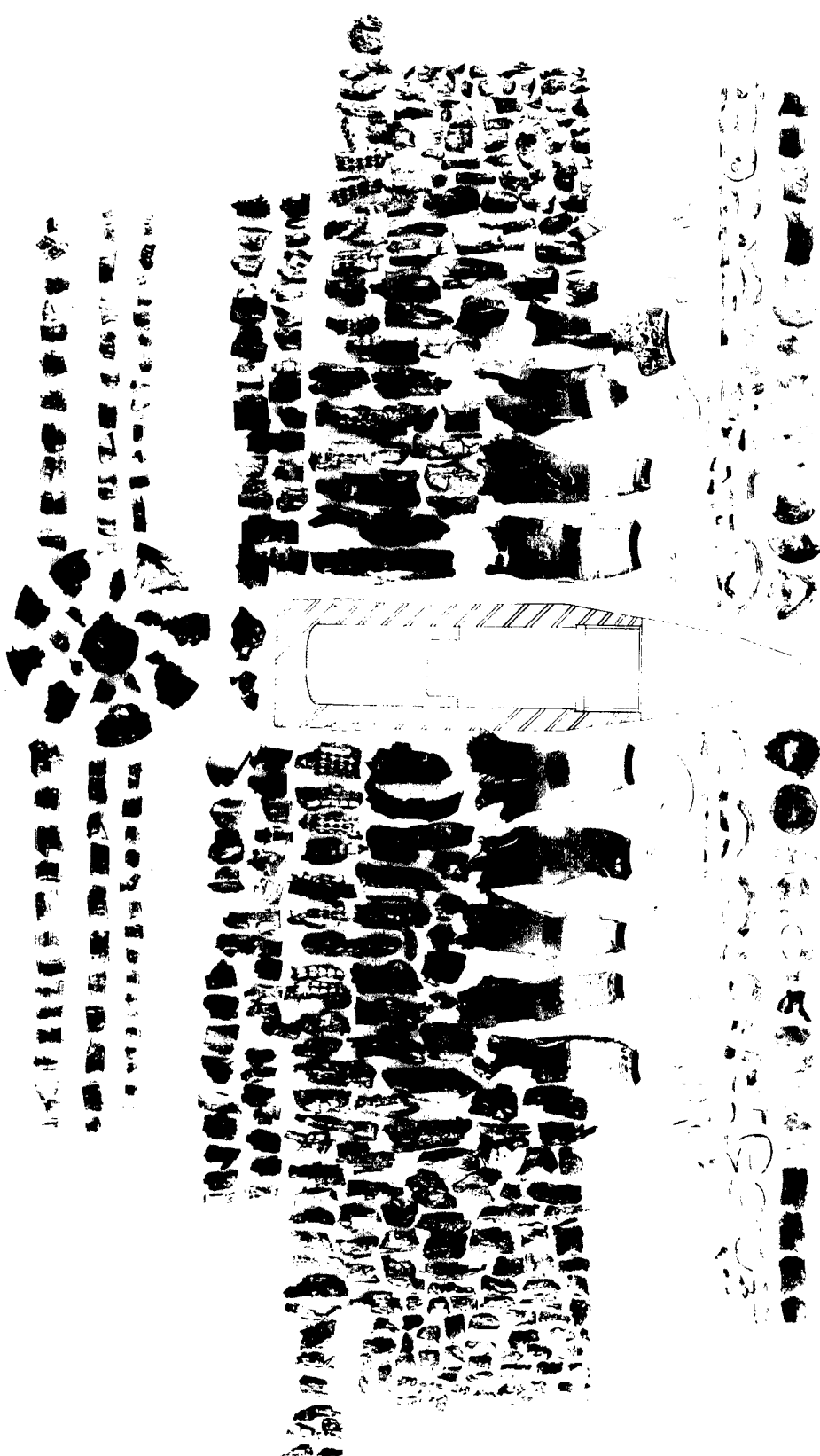


RECEIVED
JUL 10 1963

Plate 23

Shot No. 68 - Fragments of Plate 21 (Composition A-3)
rearranged to show origins.

Sh. 11 20
MAY 3-1
3 11-11-11
240-11-11-11
Musk 45-11-11



UNCLASSIFIED

OSRD
5607

DIVISION 8

NATIONAL DEFENSE RESEARCH COMMITTEE
of the
OFFICE OF SCIENTIFIC RESEARCH AND DEVELOPMENT

STUDIES OF SHELL FRAGMENT MASS DISTRIBUTION

Explosives Research Laboratory

OSRD Report No. 5607

Copy No. 29

Date: January 5, 1946

Service Projects: NO-167, OD-152

Endorsement from Dr. Ralph Connor, Chief, Division 8 to Dr. Irvin Stewart, Executive Secretary of the National Defense Research Committee. Forwarding report and noting:

"This report contains results which have been obtained in fragmenting Navy 3" A.A. shell loaded with a number of different explosives. The report also contains a detailed description of the methods used at this laboratory for collecting and analyzing the fragments produced by detonating shell. The procedure differs from that in use at certain other laboratories in this country in that the fragments are collected in sawdust and the separation from the sawdust is made magnetically.

It is brought out in the report that, even when all shell being investigated come from a single manufacturing lot, some may differ appreciably in physical properties from the others; and it is recommended that a hardness test be made on all shell before loading, so that abnormal ones can be rejected.

Most of the work has involved a comparison of TNT and Composition A3 in the 3"/50 shell, using several sizes of fuze cavity. The numbers of fragments produced having masses equal to or greater than one gram are 50-70% greater for Composition A3 than for TNT, the relative numbers varying somewhat with the size of fuze cavity.

Other reports on this subject are OSRD-5606 and 5608."

This is a progress report under Contract OEMsr-202 with the Carnegie Institute of Technology.

This document contains information affecting the national defense of the United States within the meaning of the Espionage Laws, U.S.C. 50; 31 and 32. Its transmission or the revelation of its contents in any manner to an unauthorized person is prohibited by law.

STEAP-TL

UNCLASSIFIED

UNCLASSIFIED

DISTRIBUTION

Copy Nos.

1 Dr. Irvin Stewart
2-22 OSRD Liaison Office
23-32 Office of the Chief of Ordnance, ASF, Attn: Col. S.B. Ritchie, for
SPOTM, Dr. R. O. Bengis
SPOTM, Col. I. A. Luke
SPOTM, Dr. L. R. Littleton
Picatinny Arsenal, Technical Division
Aberdeen Proving Ground, Technical Information Branch
33-47 Office of Research and Inventions, for
Chief of the Bureau of Ordnance, Res. and Dev. Division
Chief of the Bureau of Ordnance, Re2 Comdr. J.A.E. Hindman
Chief of the Bureau of Ordnance, Re2c Comdr. S. Brunauer
Naval Ordnance Laboratory
Naval Powder Factory
Naval Ordnance Test Station
48 Naval Research Laboratory
49-51 Division 3 Files
52-53 Explosives Research Laboratory Files
54 Division 3 Files
55 Dr. R. W. Cairns
56-58 Dr. G. B. Kistiakowsky
59 Dr. T. E. Lawson
60 Microfilming

Total Number of Copies - 60

UNCLASSIFIED